Nuclear IL-33 Plays an Important Role in EGFR-Mediated Keratinocyte Migration by Regulating the Activation of Signal Transducer and Activator of Transcription 3 and NF-κB

Xiuju Dai[1], Ken Shiraishi[1], Jun Muto[1], Hideki Mori[1], Masamoto Murakami[1] and Koji Sayama[1]

Nuclear IL-33 levels are high at the epidermal edges of skin wounds and facilitate wound healing. However, IL-33–mediated regulation of keratinocyte (KC) biology during wound healing remains poorly understood. During skin-wound healing, KC migration and re-epithelialization are mediated predominantly by EGFR signaling activation and depend on the function of signal transducer and activator of transcription 3 (STAT3). We found that migrating KCs at the leading edges of mouse skin wounds exhibited concomitant induction and nuclear colocalization of IL-33 and phosphorylated STAT3. In cultured human KCs, activation of EGFR signaling caused rapid elevation of nuclear IL-33, which directly interacts with phosphorylated STAT3, promoting STAT3 activation. In vitro KC migration and wound-healing assays revealed that high nuclear IL-33 levels were required for KC migration and wound closure. KC mobility associated with a lack of suprabasal epidermal keratins and extracellular matrix degradation mediated by matrix metalloproteinases (MMPs) control cell migration at the intracellular and extracellular levels, respectively. In EGFR-activated KCs, nuclear IL-33 mediated keratin 1 and 10 downregulation and MMP9 upregulation by promoting STAT3 activation and limited MMP1, MMP3, and MMP10 induction by suppressing NF-κB transactivation. Thus, epidermal nuclear IL-33 is involved in KC migration and wound closure by regulating the STAT3 and NF-κB pathways.

JID Innovations (2023);**3:**100205 doi:10.1016/j.xjidi.2023.100205

INTRODUCTION

IL-33 initially designated as a nuclear factor from high endothelial venules (Baekkevold et al., 2003) belongs to an increasing number of dual-function cytokines or nuclear alarmin cytokines; this group of cytokines presently comprises IL-33, IL-1α, HMGB1, IL-1F7b, and IL-16, all of which play a role in the nucleus apart from their extracellular receptors–mediated proinflammatory effects (Jiang et al., 2020; Sharma et al., 2008; Wilson et al., 2004). IL-33 is first synthesized as a precursor protein. The precursor full-length IL-33 (30 kDa), similar to IL-1α, contains an N-terminal nuclear localization signal and is constitutively expressed in the nucleus of endothelial and epithelial cells, where it affects transcription; this nuclear IL-33, as an alarmin, is rapidly secreted after cell damage or tissue injury and is readily cleaved by various inflammatory proteinases (Carriere et al., 2007; Moussion et al., 2008). Extracellular IL-33, particularly its mature form (18 kDa), is a specific ligand for the IL-1 receptor–related membrane-bound protein ST2; it is well-known that IL-33 is elevated in the serum of patients with severe atopic dermatitis (AD) and functions as a pro–T helper (Th) 2 cytokine, promoting AD-associated Th2 inflammation by binding to its specific receptor ST2 (Imai, 2019; Nabe, 2014). Nuclear IL-33, usually weakly detected in normal skin basal epidermal keratinocytes (KCs), is significantly elevated in migrating KCs at the edges of acute but not chronic wounds and is required for wound healing (Oshio et al., 2017; Sundnes et al., 2015). Nuclear IL-33 is also highly detected in the lesional epidermis of patients with chronic inflammatory skin diseases (Balato et al., 2016), in whom scratching often causes skin wounds. However, the role of nuclear IL-33 in KC biology during skin-wound healing remains unclear.

EGFR regulates many aspects of mammalian cells, including survival, migration, and proliferation (Jost et al., 2000). EGFR can be activated by its specific ligands and non–EGFR-ligand stimuli; the latter phenomenon, which not only a variety of G-protein–coupled receptor ligands but also some proinflammatory cytokines, binding to specific receptors, triggers tyrosine kinase receptor EGFR-dependent signal activation through ligand-dependent (triple membrane passing signaling pathway) or ligand-independent pathways, is termed EGFR

[1]*Department of Dermatology, Ehime University Graduate School of Medicine, Ehime, Japan*

Correspondence: Xiuju Dai, Department of Dermatology, Ehime University Graduate School of Medicine, Ehime 791-0295, Japan. E-mail: daixiuju@m.ehime-u.ac.jp

Abbreviations: AD, atopic dermatitis; Akt, protein kinase B; Ax, adenoviral vector; ECM, extracellular matrix; ERK, extracellular signal–regulated kinase; HB-EGF, heparin-binding epidermal GF; K, keratin; KC, keratinocyte; MEK, MAPK/extracellular signal–regulated kinase kinase; MMP, matrix metalloproteinase; NHEK, normal human epidermal keratinocyte; p-EGFR, phosphorylated EGFR; PI3K, phosphatidylinositol 3-kinase; p-STAT3, phosphorylated signal transducer and activator of transcription 3; siRNA, small interfering RNA; STAT3, signal transducer and activator of transcription 3; Th, T helper

Received 11 February 2022; revised 21 February 2023; accepted 27 February 2023; accepted manuscript published online XXX; corrected proof published online XXX

Cite this article as: JID Innovations 2023;3:100205

© 2023 The Authors. Published by Elsevier Inc. on behalf of the Society for Investigative Dermatology. This is an open access article under the CC BY-NC-ND license (http://creativecommons.org/licenses/by-nc-nd/4.0/).

transactivation (Wang, 2016). Triple membrane passing signaling pathway–dependent EGFR transactivation includes activation of matrix metalloproteinases (MMPs), MMP-mediated ectodomain cleavage, and release of the mature form of EGFR ligands from membrane precursors (the shedding of EGFR ligands) and subsequent ligand binding to EGFR, resulting in EGFR phosphorylation and internalization (Wang, 2016). In KCs, EGFR transactivation after non–EGFR-ligand stimuli is often dependent on MMPs-mediated shedding of heparin-binding epidermal GF (HB-EGF) (Dai et al., 2020; Pastore et al., 2008; Tokumaru et al., 2005). Upregulation of KC IL-33 in response to proinflammatory cytokines (Meephansan et al., 2013, 2012), infection (Jin et al., 2019), environmental stress (Pietka et al., 2019), or mite allergens (Dai et al., 2020) is attributable to EGFR transactivation, suggesting a close relationship between IL-33 expression and EGFR-mediated KC biology. During skin-wound healing, KC migration and proliferation (culminating in re-epithelialization) are mediated predominantly by EGFR activation (Stoll et al., 1997). *HB-EGF*, originally generated by the shedding of KC pro–HB-EGF in acute wounds (Tokumaru et al., 2000), is a vital GF of wound fluid (Marikovsky et al., 1993) and is the most inducible gene of KCs after wounding (Shirakata et al., 2000). HB-EGF exhibits a high affinity for EGFR (Kochupurakkal et al., 2005) and plays a vital role in skin-wound healing by accelerating KC migration rather than its proliferation (Shirakata et al., 2005). In this study, we treated normal human epidermal KCs (NHEKs) with HB-EGF to explore whether nuclear IL-33 was involved in HB-EGF–mediated KC migration and wound closure.

RESULTS

Rapid induction or activation of IL-33, EGFR, signal transducer and activator of transcription 3, and extracellular signal–regulated kinase in migrating KCs during wound healing

Mouse skin wounds were made to gain insight into the in vivo relationship between EGFR activation and IL-33 expression during wound healing, and the skin obtained from wound margins at different times was stained for phosphorylated EGFR (p-EGFR) and IL-33. Both p-EGFR and IL-33 were rapidly induced in migrating KCs at the leading edges of the wounds (Figure 1a). The p-EGFR staining was very distinct 1 day later after wounding but almost disappeared after 3 days (Figure 1a, p-EGFR). The IL-33 signal was detected strongly in the KC nucleus 1 day after wounding and remained well-marked even after 4 days (Figure 1a, IL-33) later compared with that of p-EGFR, indicating that IL-33 increase may be associated with EGFR activation during wound healing. Given the essential role of signal transducer and activator of transcription 3 (STAT3) and the involvement of extracellular signal–regulated kinase (ERK) in EGFR-mediated KC migration and wound healing (Sano et al., 1999; Uchiyama et al., 2019), we evaluated STAT3 and ERK activation status at wound margins. The staining of phosphorylated STAT3 (p-STAT3) was sustainedly prominent in the nucleus of migrating KCs after wounding, similar to that of the IL-33 signal (Figure 1a, p-STAT3). Induction of phosphorylated ERK occurs rapidly in both the cytoplasm and the nucleus of migrating KCs, with peaks evident 1 day after wounding, the same as for p-EGFR (Figure 1a, phosphorylated ERK). Next, the cellular localization of IL-33 and p-STAT3 in acute wounds was further identified under confocal immunofluorescence microscopy. In migrating KCs of the wound leading edge, IL33 protein was localized mainly in the nucleus and less in the cytoplasm, which is consistent with a previous report (Wulff et al., 2019), and the p-STAT3 was present in the nucleus but not in the cytoplasm, as evidenced by nuclear counterstaining with DAPI (Figure 1b). The concomitant induction and nuclear colocalization of IL-33 and p-STAT3 in migrating KCs of acute skin wounds indicated a potential correlation between IL-33 elevation and STAT3 activation during skin wound healing.

HB-EGF increases intracellular IL-33 expression in KCs through EGFR-mediated activation of the Ras/Raf/MAPK/ERK kinase/ERK and phosphatidylinositol 3-kinase/protein kinase B pathways

To investigate the role of EGFR in IL-33 expression, subconfluent NHEKs were treated with different concentrations of HB-EGF for the indicated times. HB-EGF at 30 ng/ml exerted a potent increase in *IL33* mRNA expression (Figure 2a) and IL-33 protein levels of the full-length form (30 kDa) but not the mature form (18 kDa) (Figure 2b); it also significantly facilitated KC migration (Figure 2c). The effect changed less, even after applying ~50–100 ng/ml HB-EGF to the cultures (Figure 2). In the following experiments, NHEKs were treated with 30 ng/ml HB-EGF to evaluate the effects on KC migration and related gene expression.

We further performed time-course experiments to quantify the expression levels of IL-33 in HB-EGF–treated cultures. HB-EGF rapidly stimulated *IL33* mRNA expression commencing 0.5 hours after addition and peaking (>5-fold) at 9 hours (Figure 3a) and significantly increased the protein levels of full-length IL-33 time dependently (Figure 3b). The *IL33* mRNA level decreased sharply from 9 hours to 14 hours after HB-EGF treatment (Figure 3a), probably because EGFR signaling returned to the quiescent state after a long duration of stimulation (Dai et al., 2022a), and climbed slightly again at 23 hours (Figure 3a), which should be attributed to EGFR reactivation after autoinduction and cross-induction by epidermal GF family members (Shirakata et al., 2010). Despite the increased IL-33 expression, HB-EGF stimulation could not exert IL-33 secretion (Figure 3c). Thus, the EGFR ligand HB-EGF significantly increases intracellular (but not extracellular) IL-33 levels in NHEKs.

The EGFR, ERK, p38, and STAT3 pathways mediate IL-33 expression in KCs (Meephansan et al., 2013, 2012). HB-EGF triggered rapid phosphorylation of EGFR, ERK, protein kinase B (Akt), and STAT3 (Figure 4a), indicating HB-EGF/EGFR-mediated activation of the Ras/Raf/MAPK/ERK kinase (MEK)/ERK, phosphatidylinositol 3-kinase (PI3K)/Akt, and Jak/STAT3 pathways. Although HB-EGF did not suppress *EGFR* mRNA expression (data not shown), we detected a decrease in the total EGFR protein levels after EGFR phosphorylation (Figure 4a, upper), which should be caused by the endocytic and lysosomal downregulation of EGFR, a key mechanism for shutting down signaling (Roepstorff et al., 2009). To explore the mechanism involved in IL-33 expression, we added AG1478 (a specific inhibitor of the tyrosine kinase activity of EGFR, which blocks the activation of EGFR and the following

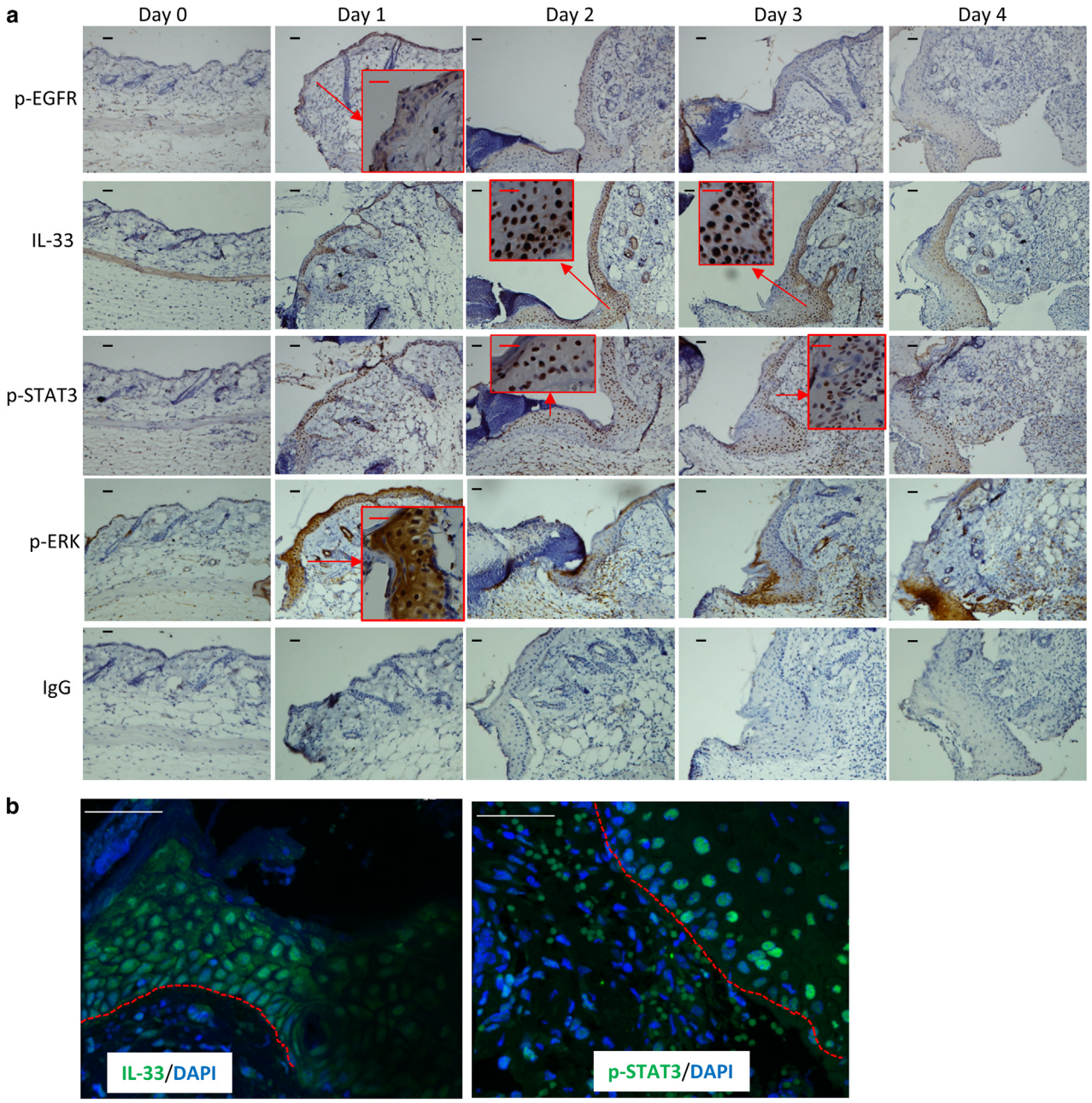

Figure 1. Rapid induction or activation of nuclear IL-33, EGFR, ERK, and STAT3 in migrating KCs during wound healing. A 6-mm circle wound on the dorsal of mice was made by a punch biopsy, and then the skins at wound margins were harvested for (**a**) paraffin or (**b**) frozen skin sections. (**a**) Immunohistochemistry of skin wound sections was performed to detect the expression and cellular localization of IL-33, p-EGFR, p-STAT3, and p-ERK in mouse skin wounds. The red boxes here show the images taken at a higher magnification, and the red arrows indicate the approximate positions at a lower magnification. Bar (black and red) = 100 mm. (**b**) The frozen mouse skin sections derived from wound margins harvested 2 days later after wounding were subjected to immunofluorescence staining of IL-33 (green) and p-STAT3 (green), with DAPI for nuclear counterstaining (blue), and the images were taken by confocal laser scanning microscope. The red broken line indicates the dermal–epidermal junction. Bar = 10 mm. The experiments were repeated three times on different days, and the results from the representative experiments are presented here. ERK, extracellular signal–regulated kinase; KC, keratinocyte; p-EGFR, phosphorylated EGFR; p-ERK, phosphorylated extracellular signal–regulated kinase; p-STAT3, phosphorylated signal transducer and activator of transcription 3; STAT3, signal transducer and activator of transcription 3.

signaling pathways), U0126 (a specific inhibitor of both MEK1 and MEK2, which inhibits the activation of MEK1/2 and ERK), or wortmannin (a selective inhibitor of PI3K, which prevents the activation of PI3K/Akt pathway) into the cultures before applying HB-EGF. AG1478 eliminated EGFR phosphorylation, inhibited ERK, Akt, and STAT3 activation (Figure 4b), and abolished HB-EGF–induced *IL33* mRNA expression (Figure 4c). U0126 significantly inhibited ERK activation (Figure 4b) and prevented IL-33 induction (Figure 4c). Wortmannin suppressed Akt activation (Figure 4b) and partially inhibited IL-33 induction (Figure 4c). To explore the role played by STAT3 activation, an adenoviral vector (Ax) bearing

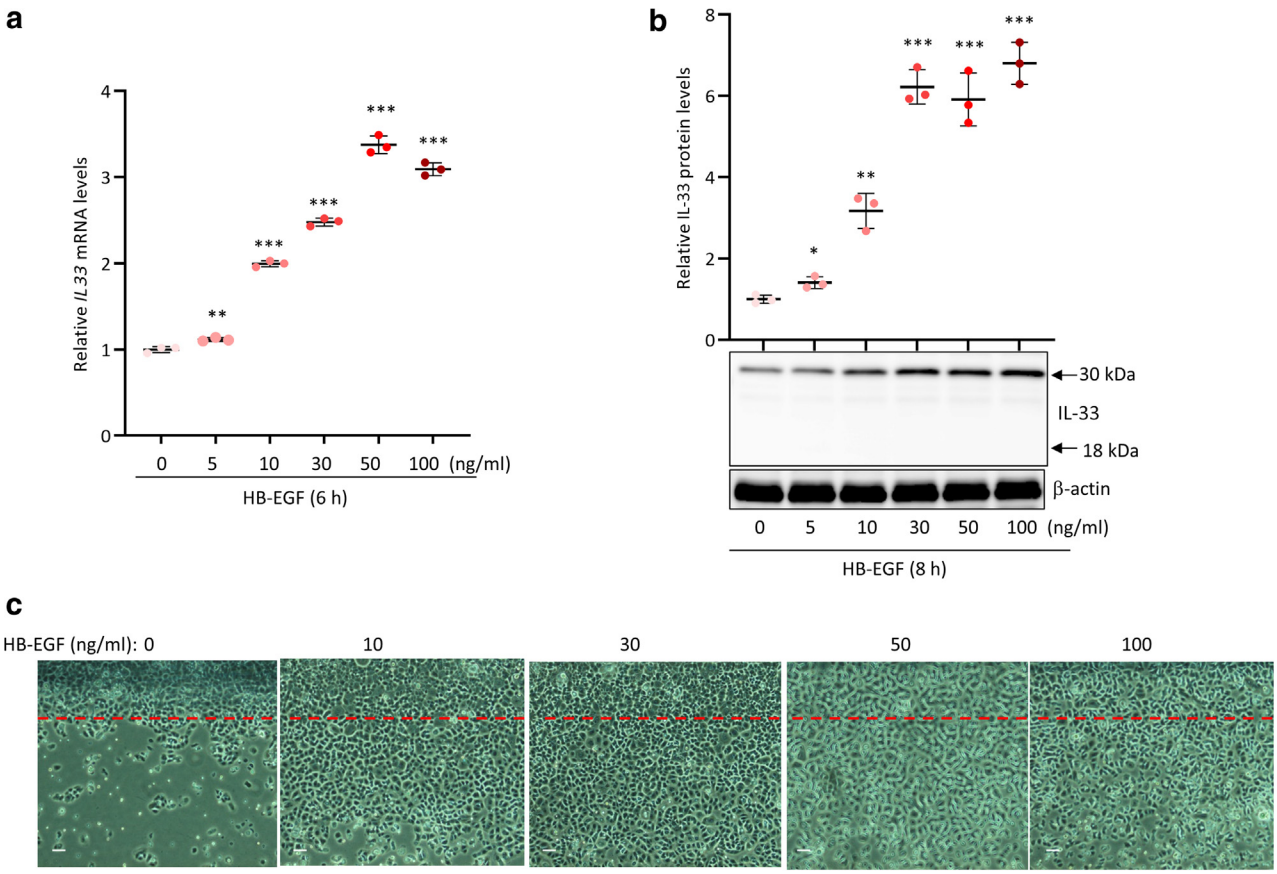

Figure 2. HB-EGF at 30 ng/ml significantly stimulates IL-33 expression and accelerates KC wound closure. (**a**) KCs were treated with different concentrations of HB-EGF for 6 hours. *IL33* mRNA expression was examined by real-time RT-PCR. The data represent the results of a single experiment with three samples per test point. (**b**) KCs were treated with different concentrations of HB-EGF for 8 hours. IL-33 protein expression was examined by western blotting. The relative IL-33 protein levels represent the ratio of IL-33 intensity in different HB-EGF–treated groups divided by that in the control group (0 ng/ml HB-EGF). The dot plot data represent the results obtained from three separate experiments. (**c**) A scrape-wound healing assay was performed in almost confluent cultures using an 8-mm scraper. The cultures were scraped, washed, and treated with different concentrations of HB-EGF. The pictures were taken 40 hours after scratching. Bar = 100 mm. All tests were repeated three times, and the results from the representative experiments are shown here. Data are shown as mean ± SD, with n = 3 for each test point. Significance was tested by one-way ANOVA (for **a** and **b**). $*P < 0.05$, $**P < 0.01$, and $***P < 0.001$ versus the control group (0 ng/ml HB-EGF). h, hour; HB-EGF, heparin-binding epidermal GF; KC, keratinocyte.

a dominant-negative form of STAT3 (STAT3F) was used to infect KCs before HB-EGF addition. STAT3F-expressing Ax eliminated STAT3 phosphorylation but did not affect IL-33 expression (Figure 4d). Thus, HB-EGF enhances IL-33 expression in NHEKs through the EGFR-activated Ras/Raf/MEK/ERK and PI3K/Akt pathways.

Nuclear IL-33 is required for HB-EGF/EGFR-mediated KC migration by interacting with p-STAT3

Next, we investigated whether intracellular IL-33 is involved in HB-EGF–mediated KC migration. We conducted a scrape-wound healing assay to evaluate KC migration and wound closure and performed the Boyden chamber migration assay to quantitate KC migration (Tokumaru et al., 2005). Cytokine IL-33 plays a role in tumor progression and cancer cell migration through the ST2–ERK pathway (Yu et al., 2015). To evaluate the involvement of IL-33/ST2 signaling in KC migration, cultures were treated with recombinant human ST2/IL-33R Fc chimera protein, a soluble decoy receptor that blocks the ability of extracellular IL-33 to signal through transmembrane ST2 in KCs (Dai et al., 2020). The addition of recombinant human ST2/IL-33R Fc chimera protein, which significantly inhibited the effect of cytokine IL-33, did not affect the induction of HB-EGF on KC migration and wound closure (Figure 5a), suggesting that IL-33/ST2 signaling is not involved in HB-EGF–mediated KC migration. Next, we investigated the role of intracellular IL-33 in KC migration. IL-33–specific small interfering RNA (siRNA) was transfected into NHEKs to deplete IL-33 expression, confirmed by the detection of *IL33* mRNA and protein (Figure 5b). As shown in Figure 5c, the scraped area became notably smaller after HB-EGF stimulation of control but not IL-33–knockdown cultures; wound closure was considerably delayed by IL-33 depletion. KC migration was further verified by Boyden chamber migration assay; HB-EGF accelerated cell migration by approximately twofold in control cultures but not in IL-33–knockdown cultures (Figure 5d). Thus, intracellular IL-33 is essential for HB-EGF–induced KC migration and wound closure.

STAT3 activation is indispensable for KC migration, and ERK activation is also involved (Sano et al., 1999). Next, we investigated whether intracellular IL-33 regulated STAT3 and ERK signaling activation. ERK and STAT3 phosphorylation during wound healing trigger their nuclear translocation and

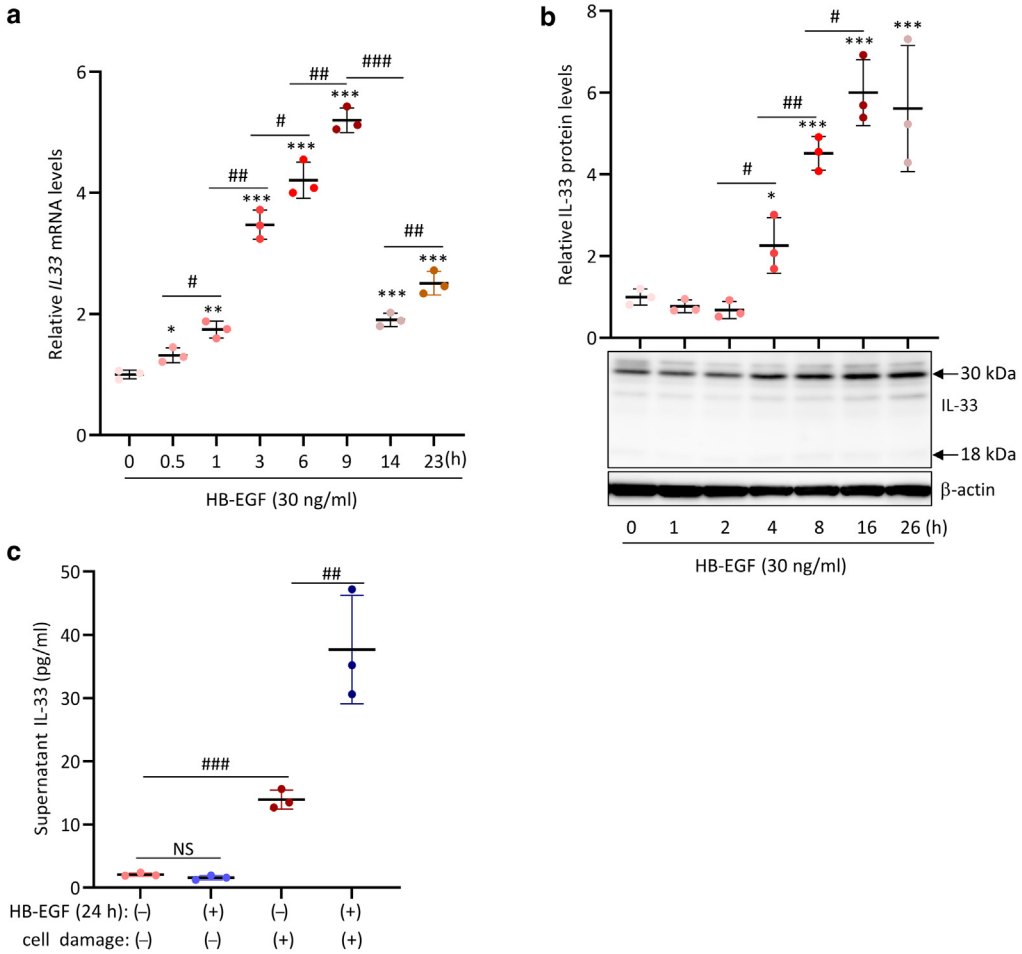

Figure 3. HB-EGF rapidly induces IL-33 expression but does not stimulate IL-33 secretion. (**a**) KCs were treated with 30 ng/ml HB-EGF for the indicated times. The levels of *IL33* mRNA were decided by real-time RT-PCR. (**b**) The levels of IL-33 protein were detected by western blotting and calculated by NIH, and the relative IL-33 protein levels represent the ratio of IL-33 intensity in different HB-EGF–treated groups divided by that in the control group (HB-EGF at 0 h). (**c**) KCs were treated with or without HB-EGF (30 ng/ml) for 24 h, cell damage was performed by scratching a lot, and the supernatants were collected for the detection of IL-33 by ELISA. All tests were repeated three times, and the results from the representative experiments are shown here. The dot blot data represents the results of a single experiment with three samples per test point (for **a** and **c**), or the dot plot data are the results of three individual experiments (for **b**). Data are shown as mean ± SD, with n = 3 for each test point. Significance was tested by one-way ANOVA (for **a** and **b**) or by a paired *t*-test (for **c**). $^{*}P < 0.05$, $^{**}P < 0.01$, and $^{***}P < 0.001$ versus the control group (HB-EGF at 0 h). $^{\#}P < 0.05$, $^{\#\#}P < 0.01$, and $^{\#\#\#}P < 0.001$ versus the indicated group. h, hour; HB-EGF, heparin-binding epidermal GF; KC, keratinocyte; NIH, National Institutes of Health; NS, not significant.

activate specific transcription factors. HB-EGF stimulated the nuclear translocation of phosphorylated ERK and p-STAT3 in KCs; IL-33 knockdown almost eliminated nuclear p-STAT3 but not phosphorylated ERK (Figure 6a). The immunoblotting of extracts from different cellular compartments showed that both IL-33 and p-STAT3 were predominately present in the nucleus but not in the cytoplasm of cultured NHEKs, particularly in the activated cells (Figure 6b); the results of confocal immunofluorescence microscopy further verified their nuclear localization in HB-EGF–activated cells (Figure 6c). Thus, HB-EGF increases the nuclear accumulation of both IL-33 and p-STAT3 in NHEKs, and the presence of nuclear IL-33 is essential for STAT3 activation. In Th2 cytokine–activated differentiated NHEKs, the association of nuclear IL-33 with p-STAT3 has been reported (Dai et al., 2022c, 2021). In cells overexpressing IL-33 and STAT3, the nuclear IL-33/p-STAT3 complexes are abundantly formed and readily detected by coimmunoprecipitation (Dai et al., 2022b). By immunoprecipitation of nuclear extracts with antibodies specific for IL-33 or p-STAT3, we observed weak coprecipitation of IL-33 and p-STAT3, indicating the formation of IL-33/p-STAT3 complexes in the nucleus of HB-EGF/EGFR-activated KCs (Figure 6d). In addition, we generated KCs expressing c-Myc–IL-33 through plasmid transfection (Figure 6e, left) and detected obvious coprecipitation of IL-33 and p-STAT3 by immunoprecipitation of nuclear extracts with antibodies specific for Myc or p-STAT3 (Figure 6e, right), further confirming the direct interaction of nuclear IL-33 and p-STAT3. Therefore, HB-EGF stimulated the formation of nuclear IL-33/p-STAT3 complexes in KCs, which is required for STAT3 nuclear translocation and activation. We further verified the requirement of STAT3 activation for HB-EGF/EGFR–mediated wound closure and KC migration (Figure 7a and b). Thus, HB-EGF accelerates KC migration and wound closure by increasing the level of nuclear IL-33, thereby promoting STAT3 activation.

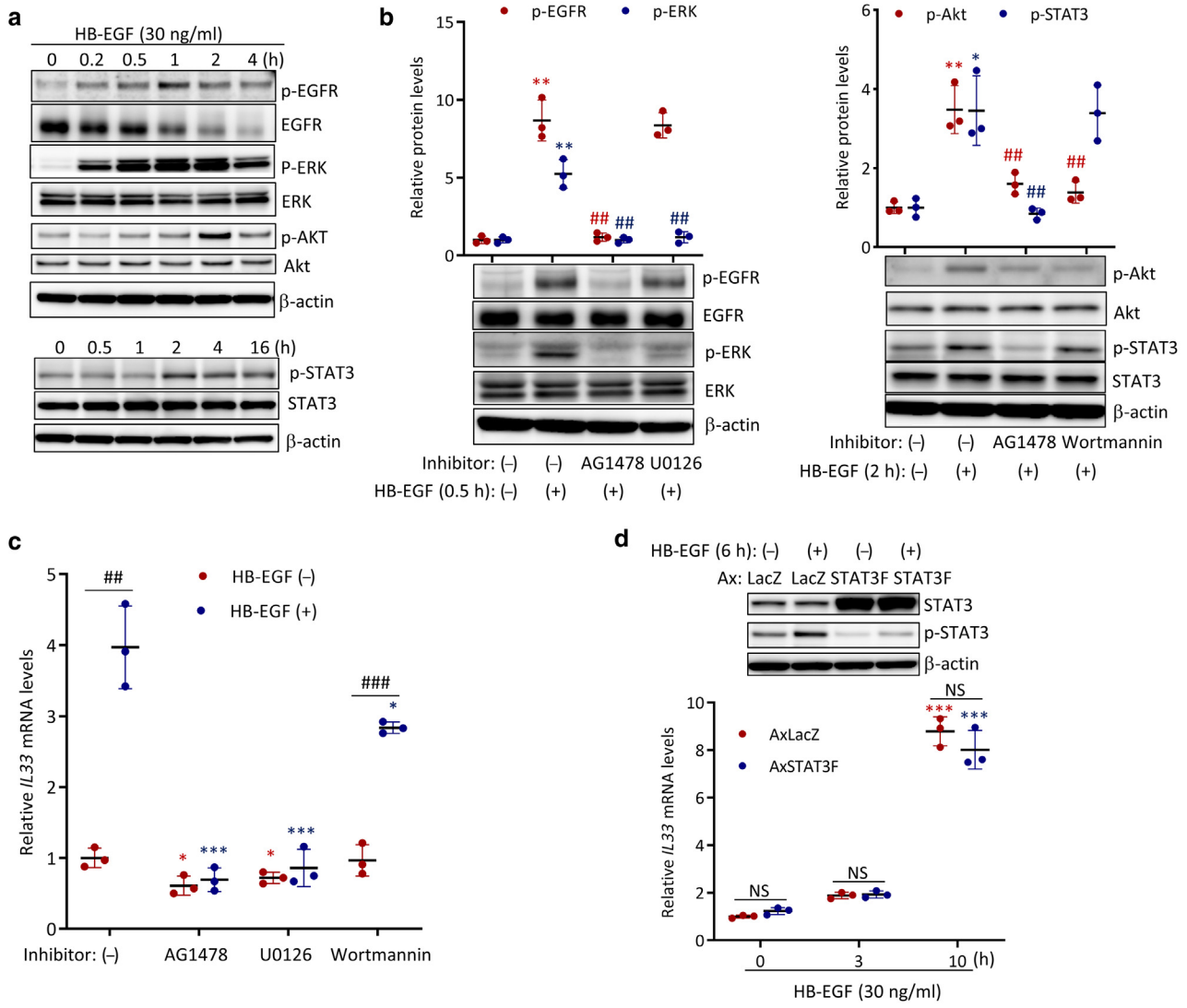

Figure 4. HB-EGF rapidly induces IL-33 expression in KCs through EGFR-mediated activation of Ras/ERK and PI3K/Akt pathways. After KCs were treated with HB-EGF (30 ng/ml) for the indicated times, (**a**) the phosphorylation of EGFR, ERK, Akt, and STAT3 and (**b**) the effects of specific inhibitors (3 mM AG1478, 10 mM U0126, or 10 mM wortmannin) on EGFR, ERK, Akt, and STAT3 activation were examined by western blotting; the relative protein levels of p-EGFR, p-ERK, p-Akt, and p-STAT3 represent the ratio of specific phosphorylated protein intensity that was corrected already by its total protein intensity in different HB-EGF (+) groups divided by that in the control group (HB-EGF [−] group) (for **b**). (**c**) KCs were pretreated with DMSO or specific inhibitors for 30 minutes and then stimulated with or without HB-EGF for 8 h, and *IL33* mRNA expression was examined by real-time RT-PCR. (**d**) KCs were infected with Ax for 24 h and then stimulated with or without HB-EGF for the indicated times; the effects of infection with STAT3F-expressing Ax on STAT3 activation and *IL33* mRNA expression were detected by western blotting and real-time RT-PCR, respectively. All tests were repeated three times, and the results from the representative experiments are shown here. The dot plot data indicate the results of three individual experiments (for **b**), or the dot blot data represent the results of a single experiment with three samples per test point (for **c** and **d**). Data are shown as mean ± SD, with n = 3 for each test point. Significance was tested by one-way ANOVA (for **b**) or two-way ANOVA (for **c** and **d**). $^{*}P < 0.05$, $^{**}P < 0.01$, and $^{***}P < 0.001$ versus HB-EGF (+)/inhibitor (−) group (for **b** and **c)** or HB-EGF at 0 h/LacZ-expressing Ax group (for **d**). $^{\#}P < 0.05$, $^{\#\#}P < 0.01$, and $^{\#\#\#}P < 0.001$ versus HB-EGF (+)/inhibitor (−) group (for **b**) or the indicated group (for **c**). Ax, adenovirus vector; Akt, protein kinase B; ERK, extracellular signal−regulated kinase; h, hour; HB-EGF, heparin-binding epidermal GF; KC, keratinocyte; NS, not significant; p-Akt, phosphorylated protein kinase B; p-EGFR, phosphorylated EGFR; p-ERK, phosphorylated extracellular signal−regulated kinase; PI3K, phosphoinositide 3-kinase; p-STAT3, phosphorylated signal transducer and activator of transcription 3; rhST, recombinant human ST; STAT3, signal transducer and activator of transcription 3.

The nuclear IL-33/p-STAT3 complex is essential for HB-EGF/EGFR-mediated induction of MMP9

The MMP family of proteins are specific extracellular matrix (ECM)−degrading enzymes that are essential for restoring tissue integrity (including epidermal wound repair) (Martins et al., 2013; Rousselle et al., 2019). KC migration is both EGFR and MMPs dependent (Stoll et al., 2010); confirming this report, we found that pretreatment with the broad-spectrum MMP inhibitor batimastat significantly suppressed HB-EGF/EGFR-mediated KC migration and wound closure (Figure 7c and d). MMP9, one of the most extensively investigated MMPs, plays a vital role in skin wound healing. *Mmp9*-knockout mice evidenced delayed wound closure (Kyriakides et al., 2009), and an MMP inhibitor or an MMP9-neutralizing antibody blocked epidermal GF−mediated KC migration in vitro (McCawley et al., 1998). In cultured

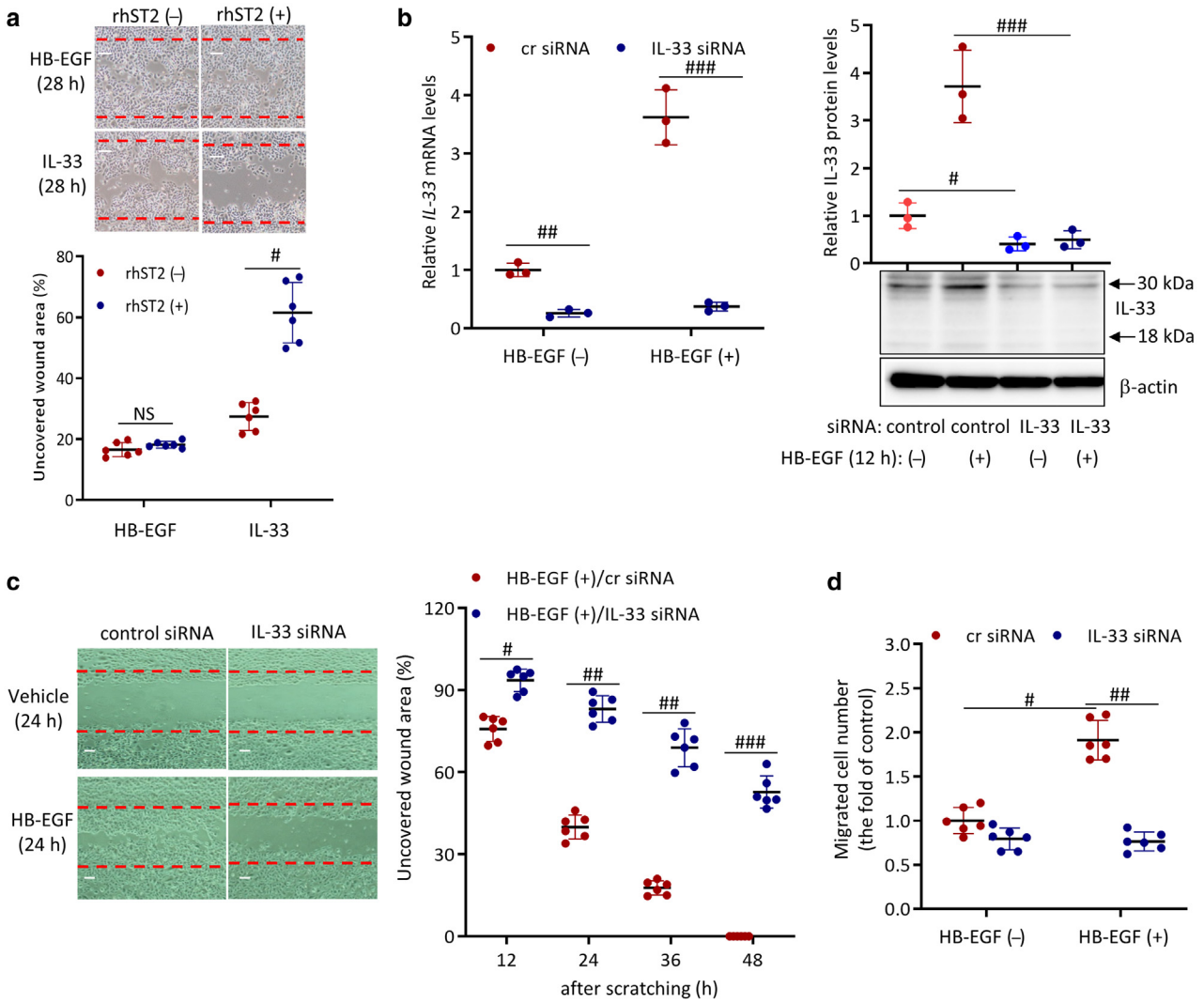

Figure 5. Nuclear IL-33 is required for HB-EGF/EGFR-mediated KC migration and wound closure. (**a**) A scratch wound healing assay was performed to evaluate the involvement of IL-33/ST2 signaling in KC migration and wound closure. After scratching wounds were made by a 6-mm scraper, the cultures were treated with HB-EGF (30 ng/ml) or mature IL-33 (100 ng/ml) together with or without recombinant human ST2/IL-33R Fc chimera protein (300 ng/ml) for 28 hours. The photos and the unrecovered wound area of several wounded spots (compared with that of the 0-hour group) calculated by ImageJ are presented here. Bar = 100 mm. (**b**) After transfection with control or IL-33 siRNA, KCs were treated with HB-EGF for 8 hours or 12 hours. *IL33* mRNA and protein expressions were detected by real-time RT-PCR and western blotting, respectively; the relative levels of *IL33* mRNA and protein are presented together with IL-33 protein bands. (**c**) After siRNA transfection, a scratch wound healing assay was performed by making wounds with a 6-mm scraper and adding HB-EGF or vehicle into cultures. The effect of IL-33 knockdown on wound closure was monitored, and the scraped area at the indicated times was quantified by ImageJ. Bar = 100 mm. (**d**) The effect of IL-33 knockdown on cell migration was quantified with a Boyden chamber migration assay. All tests were repeated three times, and the results from the representative experiments are shown here. The dot blot data represent the results of a single experiment with six (for **a**, **c**, and **d**) or three (for **b,** left) samples per test point, or the dot plot data indicate the results of three individual experiments (for **b**, right). Data are shown as mean ± SD, with n = 6 (for **a**, **c**, and **d**) or n = 3 (for **b**) for each test point. Significance was tested by a paired *t*-test (for **a**, **b,** and **c**) or two-way ANOVA (for **d**). $^{\#}P < 0.05$ and $^{\#\#}P < 0.01$ versus the indicated group. cr, control; h, hour; HB-EGF, heparin-binding epidermal GF; KC, keratinocyte; NS, not significant; siRNA, small interfering RNA.

NHEKs, HB-EGF markedly induced *MMP9* mRNA and protein expression time dependently (Figure 8a and b), coinciding with the elevation of IL-33 protein (Figure 3b). MMP9 production is regulated principally at the transcriptional level; tight regulation is critical because its expression level parallels the cell migration speed (Gordon et al., 2009; Legrand et al., 1999). A potential STAT3-binding site next to the activator protein-1 consensus sequence has been reported in the MMP9 promoter; STAT3 and activator protein-1 transcription factors cooperatively activate MMP9 transcription (Song et al., 2008). In HB-EGF–treated NHEKs, EGFR/ERK activation is essential for rapid MMP9 induction; the PI3K/Akt pathway is also involved (Figure 8c). Both STAT3 blockade and IL-33 knockdown significantly inhibited MMP9 expression, particularly in the late phases of HB-EGF treatment (Figure 8d), indicating that nuclear IL-33/p-STAT3 is involved in MMP9 induction. Next, we performed chromatin immunoprecipitation quantitative PCR using a specific antibody against p-STAT3 and specific primers for the MMP9 promoter and found that HB-EGF significantly increased p-STAT3–DNA binding in control but not in IL-33–knockdown KCs (Figure 8e). Thus, the formation of nuclear IL-33/p-STAT3

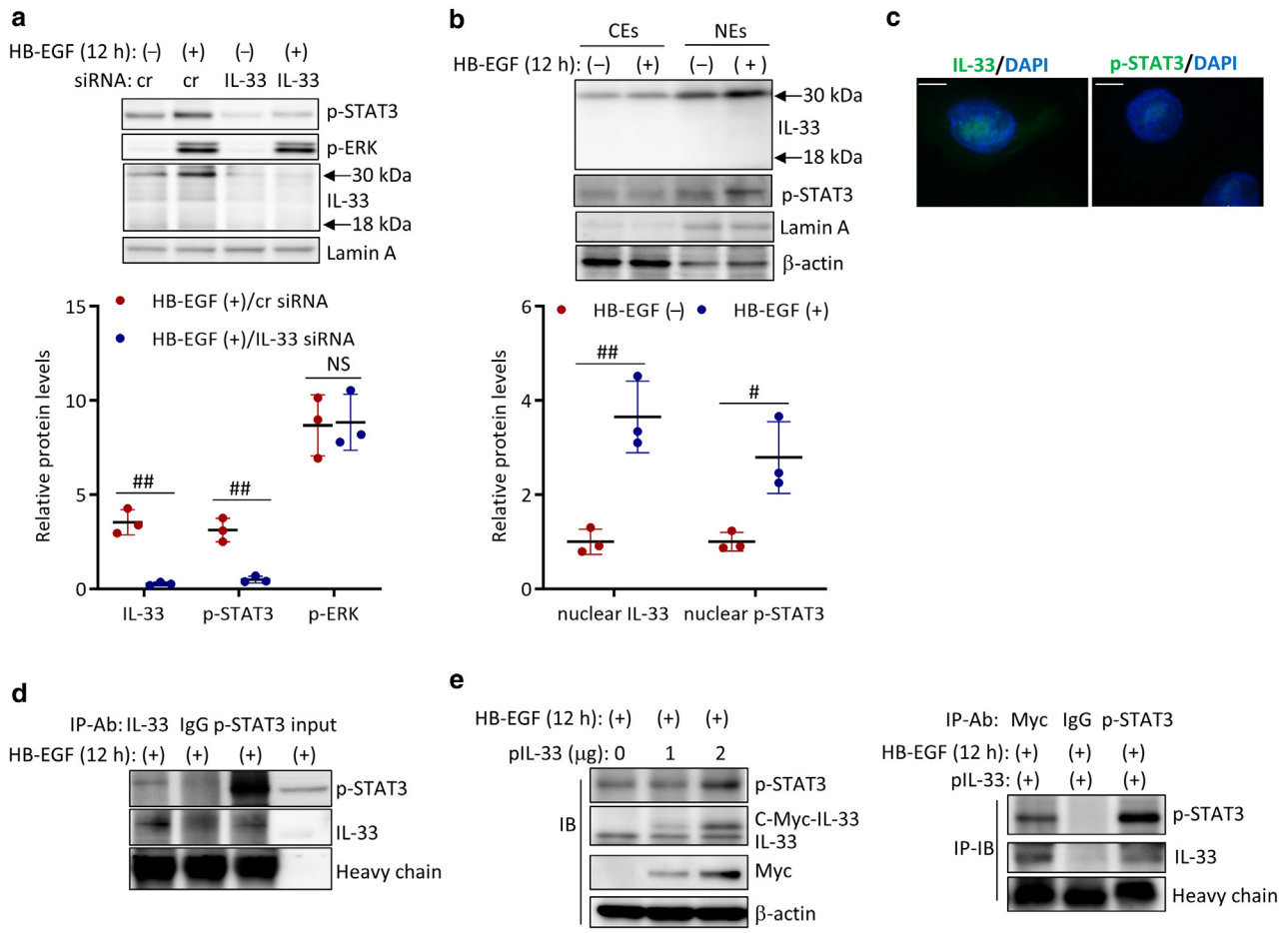

Figure 6. Nuclear IL-33 modulates STAT3 nuclear translocation and activation by integrating with p-STAT3. (**a**) KCs were transfected with siRNA for 48 h and then stimulated with HB-EGF for 12 h, and the levels of IL-33, p-STAT3, and p-ERK in nuclear extracts were detected by western blotting, and their relative quantitative levels acquired by ImageJ are presented. (**b**) After KCs were treated with or without HB-EGF for 12 h, the levels of IL-33 and p-STAT3 in CEs and NEs were detected using western blotting, and the relative quantitative levels of nuclear IL-33 and nuclear p-STAT3 were calculated by ImageJ. (**c**) After stimulating cells for 12 h, the cellular localization of IL-33 (green) and p-STAT3 (green) together with nuclear DAPI staining (blue) in HB-EGF–activated KCs was examined by confocal immunofluorescence microscopy. Bar = 10 mm. (**d**) Nuclear proteins were collected from HB-EGF (12 hours)–treated KCs, and an immunoprecipitation assay with western blotting was performed using specific antibodies for IL-33 and p-STAT3. (**e**) Subconfluent KCs were infected with pc-Myc–IL-33 (pIL-33 by 0, 1, and 2 mg plasmid per 10^6 cells for IB and 2 mg plasmid per 10^6 cells for IP–IB) for 24 hours and then stimulated with HB-EGF for 12 hours, and nuclear proteins were collected. Western blotting was performed to detect the levels of nuclear p-STAT3, IL-33, and Myc, or immunoprecipitation of Nes was performed using specific antibodies for Myc and p-STAT3 before being subjected to western blotting for the detection of p-STAT3 and IL-33. All tests were repeated three times, and the data from the representative experiments are shown here. The dot blot data indicate the results of three individual experiments. Data are shown as mean ± SD, with n = 3 for each test point. Significance was tested by paired samples *t*-test. $^{\#}P < 0.05$ and $^{\#\#}P < 0.01$ versus the indicated group. Ab, antibody; CE, cytoplasmic extract; cr, control; h, hour; HB-EGF, heparin-binding epidermal GF; IB, immunoblotting; IP, immunoprecipitation; KC, keratinocyte; NE, nuclear extract; NS, not significant; p-ERK, phosphorylated extracellular signal–regulated kinase; p-STAT3, phosphorylated signal transducer and activator of transcription 3; siRNA, small interfering RNA; STAT3, signal transducer and activator of transcription 3.

facilitates p-STAT3 nuclear translocation; in this manner, nuclear IL-33 manipulates the binding of p-STAT3 to the MMP9 promoter and promotes MMP9 transcription and expression in HB-EGF/EGFR-activated KCs.

Nuclear IL-33 represses HB-EGF/EGFR-mediated induction of MMP1, MMP3, and MMP10 by interfering with NF-κB transactivation

Apart from MMP9, HB-EGF significantly increased the expression levels of MMP1, MMP3, and MMP10, with similar patterns (Figure 9a), but did not affect the expression of other MMPs (data not shown). The mRNA levels of the three MMPs peaked 7 hours after stimulation and then gradually decreased (Figure 9a), accompanied by a notable elevation in IL-33 protein levels (Figure 3b). In HB-EGF–treated NHEKs, EGFR/ERK activation was essential for their rapid induction, and PI3K/Akt pathway was also involved (Figure 9b). STAT3 inactivation partially suppressed the expression of all the three MMPs (Figure 9c); however, IL-33 knockdown augmented the mRNA levels of *MMP1*, *MMP3*, and *MMP10*, particularly in the late phase, by ∼1.7-fold, 4.6-fold, and 4.5-fold, respectively (Figure 9d). According to a previous report (Ali et al., 2011), nuclear IL-33 can interact with the transcription factor NF-κB to reduce NF-κB–mediated gene expression. In IFN-γ–activated KCs, nuclear IL-33 inhibited IL-8 expression by suppressing NF-κB activation (Meephansan et al., 2012). Although overexpressed full-length IL-33 directly interacted with endogenous p65 and p50 in IL-1β–activated cells (Ali

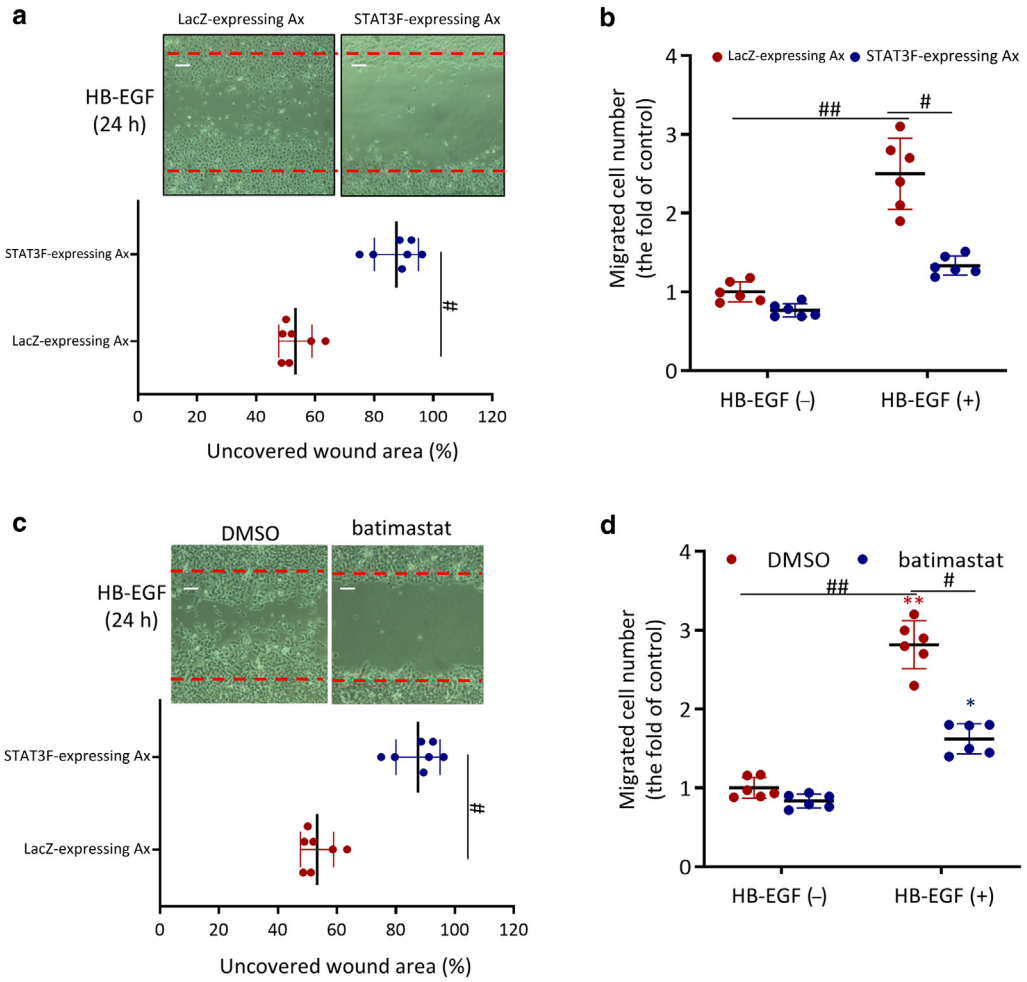

Figure 7. STAT3 and MMPs are involved in HB-EGF–accelerated KC migration and wound closure. (**a**) KCs were infected with Ax for 24 hours and then stimulated with HB-EGF for 15 or 24 hours; the effects of STAT3 inactivation on KC migration and wound closure were investigated by scratch-wound healing assay (wounds were made by an 8-mm scraper; the unrecovered wound area was quantified by ImageJ), and (**b**) the migrated cells were calculated with a Boyden chamber migration assay. After stimulating cells for 24 hours, a scratch-wound healing assay (wounds were made by an 8-mm scraper; the unrecovered wound area was quantified by ImageJ) and a Boyden chamber migration assay were performed to evaluate the effects of MMP inhibitor batimastat (10 mM) on (**c**) HB-EGF–mediated wound closure and (**d**) KC migration, respectively. All tests were repeated three times, and the data from the representative experiments are shown here. The dot blot data represent the results of a single experiment with six samples per test point. Data are shown as mean ± SD, with n = 6 for each test point. Significance was tested by paired samples *t*-test (for **a** and **c**) or two-way ANOVA (for **b** and **d**). $^{*}P < 0.05$ and $^{**}P < 0.01$ versus the relative HB-EGF (–) group (for **d**). $^{\#}P < 0.05$ and $^{\#\#}P < 0.01$ versus the indicated group. Bar = 100 mm (for **a** and **c**). Ax, adenovirus vector; h, hour; HB-EGF, heparin-binding epidermal GF; KC, keratinocyte; MMP, matrix metalloproteinase; STAT3, signal transducer and activator of transcription 3.

et al., 2011), we failed to evidence the coprecipitation between IL-33 and NF-κB proteins in HB-EGF–activated NHEKs (data not shown). However, NF-κB transactivation was significantly increased by IL-33 knockdown, as detected by the electrophoretic mobility shift assay (Figure 9e). Next, KCs were transfected with nanoLuc reporter vector with NF-κB response element, and a reporter assay was performed. As shown in Figure 9f, IL-33 knockdown significantly increased the NF-κB–responsive luciferase activity, particularly in HB-EGF–activated KCs (Figure 9f). These data indicated that nuclear IL-33 prevented NF-κB transactivation in activated KCs. Bay11-7082 (Figure 9g), a specific inhibitor of NF-κB, and p65 depletion (Figure 9g) eliminated the IL-33 knockdown–induced increases in MMP1 and MMP10 and partially suppressed IL-33 knockdown–dependent MMP3 upregulation (Figure 9h). Therefore, nuclear IL-33 restrains the HB-EGF/EGFR-mediated upregulation of MMP1, MMP3, and MMP10 by suppressing NF-κB transactivation.

Nuclear IL-33 downregulates the expression levels of suprabasal epidermal keratins

The principal initial effect of HB-EGF on wound healing is the induction of cell motility, which is associated with altered KC differentiation, in particular, inhibition of the expression of suprabasal epidermal keratins (Poumay and de Rouvroit, 2012; Shirakata et al., 2005). HB-EGF downregulated keratin (K) 10 production in cultured KCs; K10 was absent from the migrating epidermal margins of skin wounds (Mathay et al., 2008). In acute skin wounds of mice, we found that both K1 and K10 expressions were suppressed in the regenerating epidermis, particularly 2 or 3 days after wounding (Figure 10a) when nuclear IL-33 and p-STAT3 stained

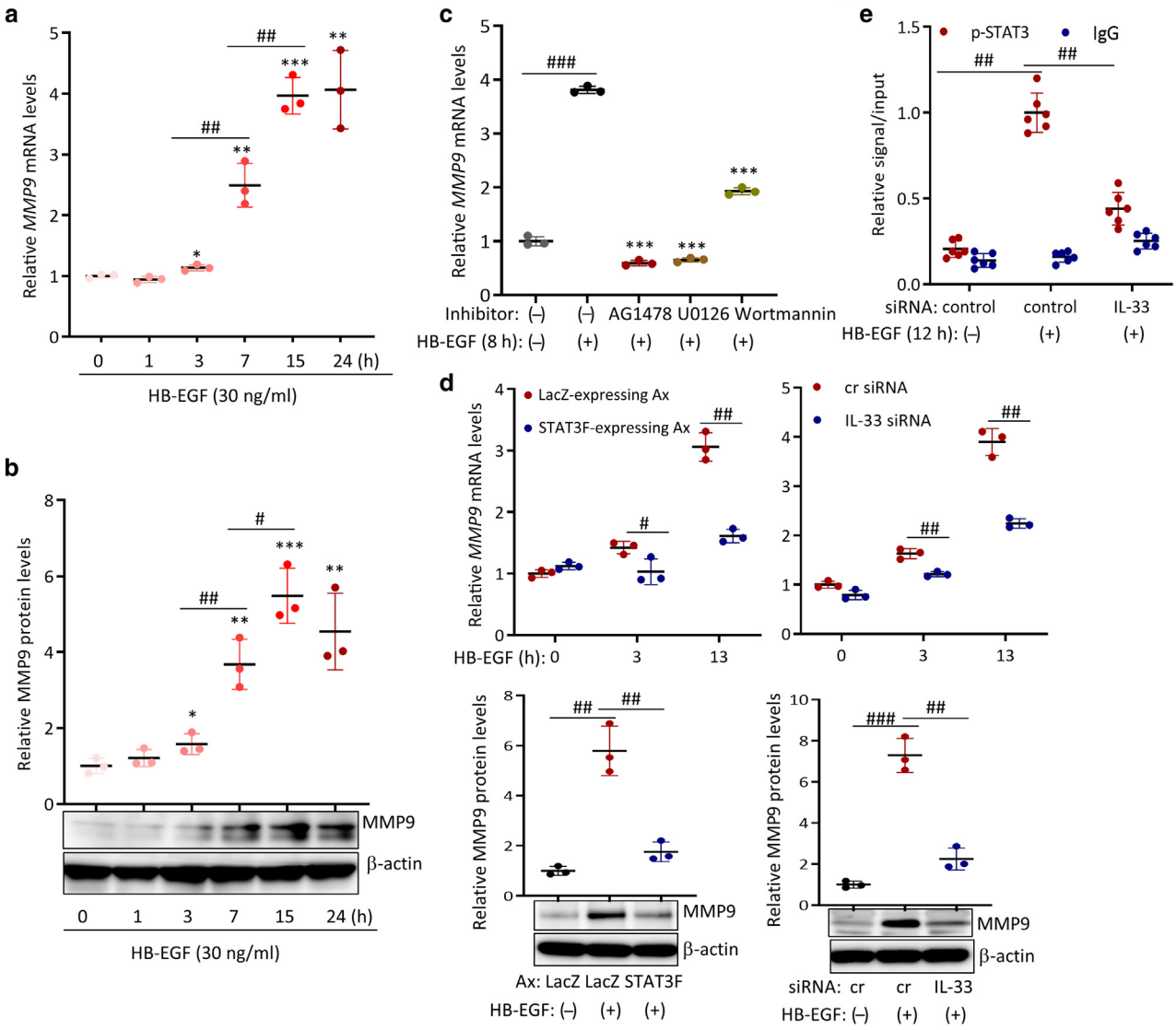

Figure 8. The nuclear IL-33/p-STAT3 complex is essential for EGFR-mediated induction of MMP9. KCs were stimulated with HB-EGF (30 ng/ml) for the indicated times, and (**a**) *MMP9* mRNA expression and (**b**) MMP9 protein expression were detected by real-time RT-PCR and western blotting, respectively. (**b**) The relative MMP9 protein levels represent the ratio of the band intensity in different HB-EGF–treated groups divided by that in the control group (HB-EGF at 0 hours). (**c**) KCs were pretreated with or without a specific inhibitor and then stimulated with HB-EGF for 8 hours, and *MMP9* mRNA expression was checked by real-time RT-PCR. (**d**) KCs were infected with Ax or transfected with siRNA and then stimulated with HB-EGF for ~0–13 hours (RNA) or 18 hours (protein). *MMP9* mRNA and protein levels were determined by real-time RT-PCR and western blotting, respectively, and the relative MMP9 protein levels represent the ratio of the band intensity in different HB-EGF–treated groups divided by that in the HB-EGF (–) group. (**e**) KCs were transfected with siRNA and then stimulated with HB-EGF for 12 hours. The cells were subjected to a ChIP-qPCR assay using a specific antibody for p-STAT3 and specific primers for the MMP9 promoter. All tests were repeated three times, and the data from the representative experiments are shown here. The dot blot data represent the results of a single experiment with (**a**, **c**, **d**) three (mRNA) or (**e**) six samples per test point, or the dot blot data indicate the results of three individual experiments (for **b** and **d**) (protein). Data are shown as mean ± SD, with n = 3 (for **a**–**d**) or with n = 6 (for **e**) for each test point. Significance was tested by one-way ANOVA (for **a**, **b**, and **c**) or a paired *t*-test (for **d** and **e**). $^{*}P < 0.05$, $^{**}P < 0.01$, and $^{***}P < 0.001$ versus the HB-EGF at 0 h group (for **a** and **b**) or the HB-EGF (+)/inhibitor (–) group (for **c**). $^{\#}P < 0.05$, $^{\#\#}P < 0.01$, and $^{\#\#\#}P < 0.001$ versus the indicated group. Ax, adenovirus vector; ChIP, chromatin immunoprecipitation; cr, control; h, hour; HB-EGF, heparin-binding epidermal GF; KC, keratinocyte; MMP9, matrix metalloproteinase 9; p-STAT3, phosphorylated signal transducer and activator of transcription 3; siRNA, small interfering RNA; STAT3, signal transducer and activator of transcription 3.

strongly. In cultured NHEKs, HB-EGF significantly decreased the *K1* and *K10* mRNA and protein expression levels in a time-dependent manner (Figure 10b). STAT3 inactivation nearly rescued the expression of suprabasal epidermal keratins (K1 and K10) suppressed by HB-EGF (Figure 10c and d), and IL-33 knockdown partially restored their mRNA and protein levels (Figure 10e and f). Thus, EGFR-mediated downregulation of suprabasal epidermal keratin expression is at least partially attributable to the action of the nuclear IL-33/p-STAT3 complex.

DISCUSSION

Re-epithelialization, which initiates the closure of skin wounds, involves KC migration, proliferation, and differentiation; migration is one of the earliest and most important events determining the efficiency of overall wound repair.

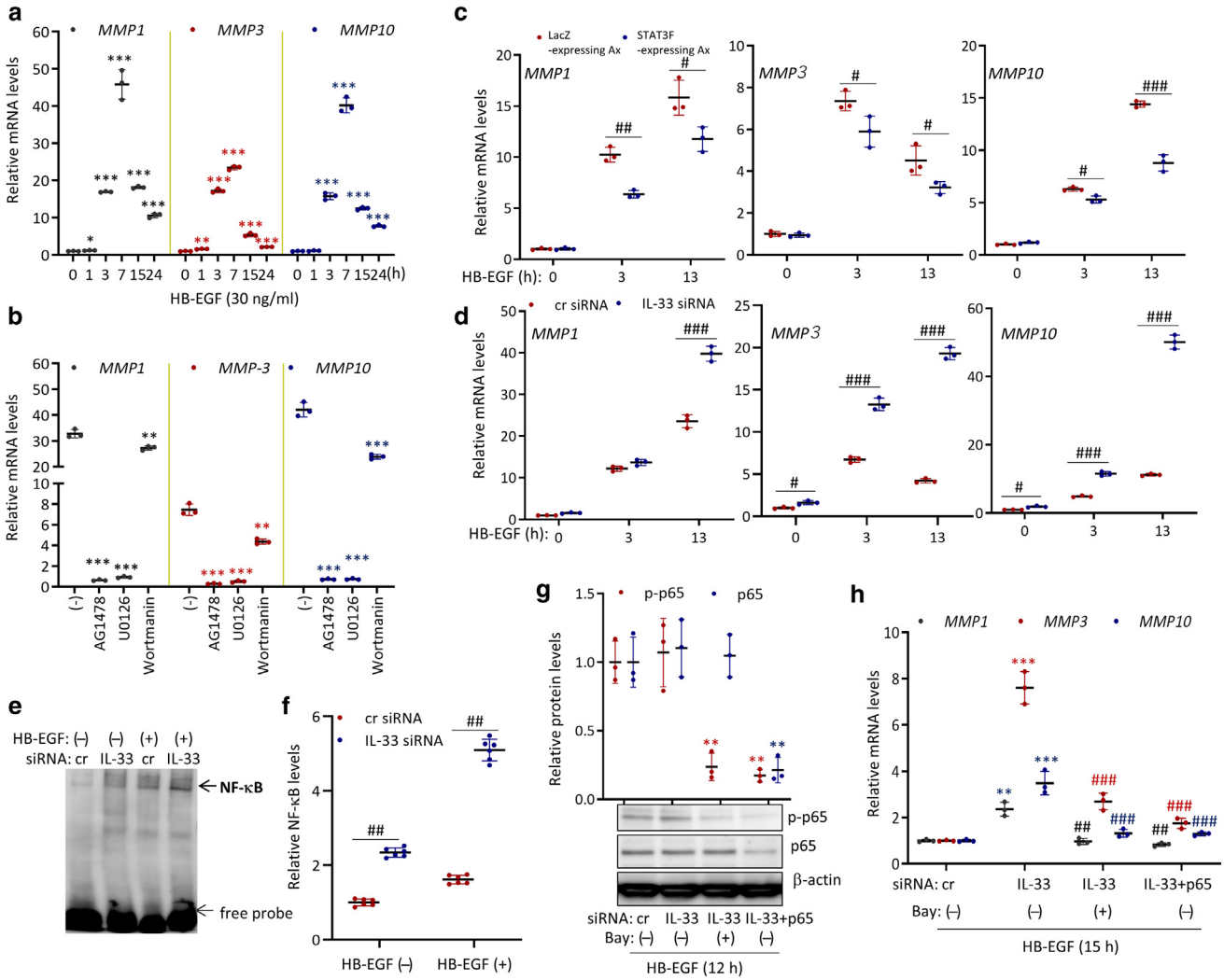

Figure 9. Nuclear IL-33 restrains EGFR-mediated upregulation of MMP1, MMP3, and MMP10. KCs were pretreated with inhibitors or without inhibitors and then stimulated with HB-EGF for the (**a**) indicated times or (**b**) 8 hours; the mRNA expression levels of *MMP1*, *MMP3*, and *MMP10* were detected by real-time RT-PCR. KCs were (**c**) infected with Ax or (**d**) transfected with siRNA and then stimulated with HB-EGF for ∼0−13 hours, and the samples were collected and subjected to real-time RT-PCR for the detection of *MMP* mRNA. (**e**) KCs were transfected with siRNA, treated with HB-EGF for 12 hours, and collected for EMSA to evaluate NF-κB transactivation. (**f**) KCs were transfected with siRNA and infected with a plasmid expressing pNL3.2.NF-κB-RE vector and then treated with HB-EGF for 12 hours, the cells were collected, and a reporter assay was performed to detect NF-κB−responsive luciferase activity. KCs were transfected with siRNA, treated with or without Bay11-7082 (10 mM), and then exposed to HB-EGF for 12 or 15 hours, and the cells were collected to evaluate (**g**) the expression of p65 and p-p65 (with western blotting) and (**h**) the effects of NF-κB inhibition or p65 depletion on *MMP* mRNA (with real-time RT-PCR). (**g**) The protein bands were quantified and corrected; the relative protein levels compared with those of the control group are presented here. All tests were repeated three times, and the data from the representative experiments are shown here. The dot blot data represent the results of a single experiment with three (for **a**, **b**, **c**, **d,** and **h**) or six (for **f**) samples per test point, or the dot blot data indicates the results of three individual experiments (for **g**). Data are shown as mean ± SD, with n = 6 (for **f**) or n = 3 (for the others) for each test point. Significance was tested by one-way ANOVA (for **a**, **b**, **g**, and **h**) or a paired *t*-test (for **c**, **d**, and **f**). $^{*}P < 0.05$, $^{**}P < 0.01$, and $^{***}P < 0.001$ versus (**a**) the relative HB-EGF 0-hour group, (**b**) the relative HB-EGF (+)/inhibitor (−) group, or (**g, h**) the relative Bay11-7082 (−)/control siRNA group. $^{\#}P < 0.05$, $^{\#\#}P < 0.01$, and $^{\#\#\#}P < 0.001$ versus the indicated group (for **c**, **d**, and **f**) or the relative Bay11-7082 (−)/IL-33 siRNA group (for **h**). Bay denotes Bay11-7082. Ax, adenovirus vector; cr, control; EMSA, electrophoretic mobility shift assay; h, hour; HB-EGF, heparin-binding epidermal GF; KC, keratinocyte; MMP, matrix metalloproteinase; p-p65, phosphorylated p65; siRNA, small interfering RNA.

Therefore, an understanding of the signaling involved in KC migration is important. IL-33 is predominantly expressed in the nucleus of barrier endothelial and epithelial cells (Moussion et al., 2008), suggestive of a role in injury repair. Using primary KCs cultured in monolayers, we determined that HB-EGF induces rapid elevation of full-length IL-33 in the nucleus and formation of the nuclear IL-33/p-STAT3 complex. The elevated nuclear IL-33 mediated MMP9 upregulation and K1 and K10 downregulation by promoting STAT3 activation and limited MMP1, MMP3, and MMP10 production by suppressing NF-κB transactivation, all of which are important in terms of KC migration. This study clarified that nuclear factor IL-33 but not IL-33/ST2 signaling is required for HB-EGF/EGFR-mediated KC migration and wound closure. Except for its marked nuclear accumulation, IL-33 was weakly detected in the cytoplasm of migrating KCs in vivo; the transient cytoplasmic localization of IL-33 can come from its continuous synthesis or imminent extracellular

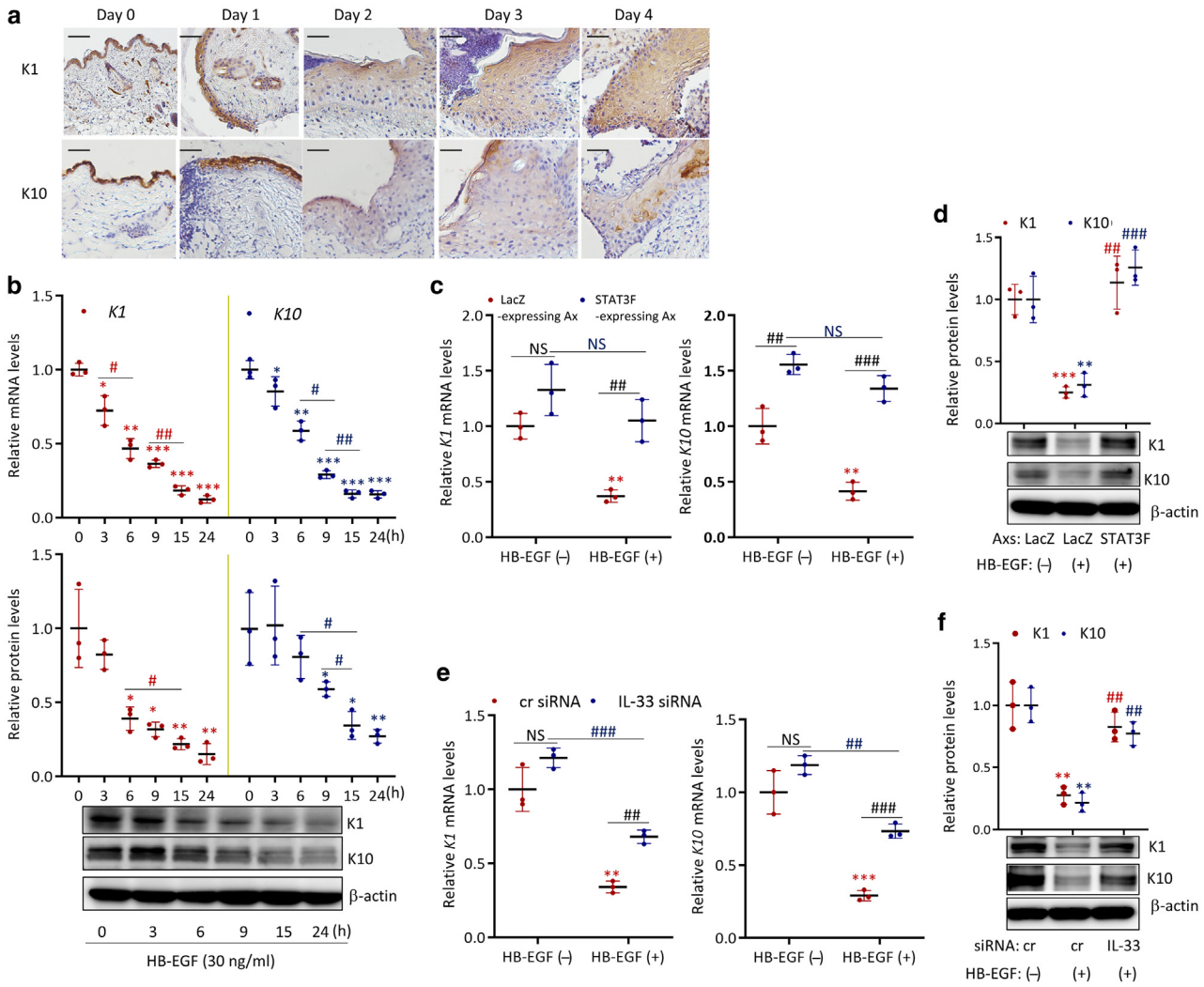

Figure 10. The nuclear IL-33/p-STAT3 complex is responsible for the suppression of K1 and K10. (**a**) Skin sections obtained from the margins of mice wounds were subjected to immunohistochemistry to detect K1 and K10. Bar = 100 mm. (**b**) KCs were treated with HB-EGF for the indicated times, or (**c, d**) KCs were infected with Ax or (**e, f**) transfected with siRNA and then stimulated with HB-EGF for 13 hours, and the mRNA and protein levels of K1 and K10 were determined by real-time RT-PCR and western blotting, respectively. (**b**, **d**, **f**) The relative quantitative levels of K1 and K10 proteins were decided by ImageJ. All tests were repeated three times, and the data from the representative experiments are shown here. The dot blot data represent the results of a single experiment with three samples per test point (for **b** [mRNA], **c**, and **e**), or the dot blot data indicates the results of three individual experiments (for **b** [protein], **d**, and **f**). Data are shown as mean ± SD, with n = 3 for each test point. Significance was tested by one-way ANOVA (for **b**), two-way ANOVA (for **c** and **e**), or a paired *t*-test (for **d** and **f**). $^{*}P < 0.05$, $^{**}P < 0.01$, and $^{***}P < 0.001$ versus the relative HB-EGF 0-hour group (for **b**) or the relative HB-EGF (−) group (for **c**–**f**). $^{\#}P < 0.05$, $^{\#\#}P < 0.01$, and $^{\#\#\#}P < 0.001$ versus the indicated group (for **b**, **c**, and **e**) or the relative HB-EGF (+)/LacZ-expressing Ax or control siRNA group (for **d** and **f**). Ax, adenovirus vector; cr, control; HB-EGF, heparin-binding epidermal GF; K, keratin; KC, keratinocyte; NS, not significant; siRNA, small interfering RNA; STAT3, signal transducer and activator of transcription 3.

secretion after tissue injury (Wilson et al., 2004), which should not be important for KC migration.

In cultured KCs, HB-EGF (in this study) and non−EGFR-ligand stimuli (cytokines and mite allergens) (Dai et al., 2020; Meephansan et al., 2013, 2012) increased the expression of nuclear IL-33 mainly through EGFR-mediated ERK activation, suggesting that EGFR/ERK activation, regardless of the stimulus, is commonly involved in IL-33 transcription. During wound healing, STAT3 activation is essential not only for EGFR ligand−mediated KC migration but also for cell migration induced by non−EGFR-ligand stimuli, including mechanical stress (Stoscheck et al., 1992), nucleotides (Block et al., 2011; Boucher et al., 2011; Stoscheck et al., 1992; Yin et al., 2007), cytokines (Cheng et al., 2010; Gallucci et al., 2004), and antimicrobial peptides (Niyonsaba et al., 2007; Tokumaru et al., 2005), most of which trigger EGFR transactivation. Several migration stimuli increased IL-33 expression (through EGFR transactivation) in KCs (Dickel et al., 2010; Meephansan et al., 2013) and fibroblasts (Nomura et al., 2012). In this study, we found that the HB-EGF/EGFR/ERK/nuclear IL-33 pathway enhanced KC migration principally through the maintenance of STAT3 activation. It is reasonable to suggest that nuclear IL-33 contributes to non−EGFR-ligand stimuli promoting cell migration. The associations between non−EGFR-ligand stimuli and nuclear IL-33 in terms of accelerating cell migration and wound healing require further study.

Cytokines and GFs that upregulate IL-33 expression in cultured KCs are produced in response to inflammation and

damage of the epidermis of patients with AD or psoriasis; the mediators include certain Th1, Th2, and Th17 cytokines (Dai et al., 2022c, 2021; Meephansan et al., 2013, 2012; Savinko et al., 2012; Vageli et al., 2015) and EGFR ligands, especially HB-EGF (Mathay et al., 2011). Nuclear IL-33 and p-STAT3 levels are high in the affected epidermis of such patients (Balato et al., 2016; Fukushi et al., 2011). Scratching, infection, and inflammation often cause minor wounds or injuries; therefore, wound repair occurs continuously in such inflammatory skin. In Th2-activated differentiated KCs (equivalent to the upper-layer epidermal cells of AD lesions), nuclear IL-33/p-STAT3 suppressed the levels of differentiation markers (especially FLG) (Dai et al., 2022c, 2021). Therefore, the nuclear IL-33/p-STAT3 elevation in the upper-layer epidermis of AD lesions likely contributes to skin barrier dysfunction by impairing cellular differentiation. In the basal and suprabasal layers of inflammatory lesions characterized by poor differentiation and epidermal hyperplasia, as are wound margins, the enhanced nuclear IL-33/STAT3 activation may facilitate wound repair by promoting KC migration. Thus, by serving as a transcriptional cofactor or regulator of STAT3, nuclear IL-33 appears to regulate differences in KC biology under certain cellular conditions and distinct local inflammation.

KC migration is governed by a balanced dynamic interaction between cells and the ECM. After wounding, activated KCs at the wound edge undergo dramatic morphological changes accompanied by upregulated expression of MMPs. In humans, MMPs play key roles in cellular migration by catabolizing ECM components; specific MMPs are confined to particular wound locations and are expressed only during certain stages of wound repair, thus playing crucial roles in rapid KC migration and appropriate re-epithelialization (Martins et al., 2013). HB-EGF/EGFR significantly induced the expression of MMP1, MMP3, MMP9, and MMP10 in NHEKs. In normal skin wounds, MMP1, MMP9, and MMP10 were rapidly induced after wounding in migrating KCs at the leading edge but became undetectable after re-epithelialization (Martins et al., 2013). The regulation of nuclear IL-33 on these MMPs and its rapid elevation in migrating KCs after wounding indicate the involvement of nuclear IL-33 in the initiation of skin wound healing. During wound healing, MMP9 produced by migrating KCs usually persists for several weeks until the wound heals and degrades basal membrane collagen IV and laminins, allowing KCs to migrate over the wound, MMP1 triggers KC migration through interactions with a2b1 integrin and type I collagen, and MMP10 stimulates KC migration principally by degrading various collagenous and noncollagenous connective tissue macromolecules (Martins et al., 2013). Although MMP3 and MMP10, also termed stromelysin-1 and stromelysin-2, respectively, similarly affect ECM degradation, the MMPs are distinct. MMP3 is expressed by proliferating cells adjacent to a wound leading edge. Apart from matrix degradation, MMP3 is a potent activator of several pro-MMPs, particularly pro-MMP9; it also plays a significant role in wound contraction regulation by controlling the formation of organized actin bundles within dermal fibroblasts (Martins et al., 2013). MMP-mediated ECM degradation facilitates KC migration; however, excessive MMP activity, a feature of chronic wounds, causes excessive matrix degradation, preventing wound healing (Martins et al., 2013). Transcription factors NF-κB, STAT3, and activator protein-1 have been shown to mediate the expression of various MMPs (Kajanne et al., 2007; Na et al., 2016; Xiang et al., 2019). In HB-EGF–treated KCs, EGFR/ERK activation, which causes activator protein-1 transactivation, mediated rapid induction of MMPs; the nuclear IL-33/p-STAT3 complex was required for upregulation of MMP9, whereas nuclear IL-33–dependent inhibition of NF-κB transactivation, probably because of impaired NF-κB p65 binding to its cognate DNA (Ali et al., 2011), not only suppressed MMP1, MMP3, and MMP10 expression but also suppressed MMP9 function by reducing the MMP3 level, thus avoiding excessive ECM degradation. Therefore, during wound repair, epidermal nuclear IL-33 regulates KC migration and may also affect fibroblast function by controlling MMP3 expression. During wound healing, an elevated HB-EGF level is always accompanied by reduced levels of suprabasal keratins in migrating KCs (Stoll et al., 2012). Similar histological findings have been reported in the lesional epidermis of patients with AD and those with psoriasis (Mathay et al., 2011), in whom skin repair follows scratching or inflammation. It seems that a lack of suprabasal epidermal keratins at the leading edge of a wound or in inflammatory lesions is a prerequisite for cell mobility. Our findings in this and previous studies (Dai et al., 2022c, 2021) imply that the nuclear IL-33/p-STAT3 complex likely mediates the suppression of K1 and K10 in regenerating epidermis. Therefore, nuclear IL-33 probably affects KC migration by regulating ECM degradation and facilitating cell mobility.

Oshio et al. (2017) found that nuclear IL-33 suppressed skin inflammation and thereby promoted wound healing by controlling NF-κB activation to reduce the production of proinflammatory cytokines, as revealed by studies on *Il33*-knockout mice. Local inflammation affects KC migration and wound closure in normal skin. In in vitro/ex vivo wound-healing models, re-epithelialization proceeds in two steps through simple migration and subsequent proliferation of KCs, unaffected by the inflammation (Heilborn et al., 2003). We did not detect significant upregulation of proinflammatory cytokines in HB-EGF–treated NHEKs, regardless of IL-33 expression (data not shown). Therefore, in in vitro wound-healing model, inflammation is not the target of nuclear IL-33 in accelerating KC migration. However, in normal skin wounds, nuclear IL-33 expressed in migrating KCs through the inhibition of NF-κB transactivation could prevent excessive matrix degradation–caused skin inflammation, thereby facilitating wound healing.

Therefore, nuclear full-length IL-33 acts as an essential transcriptional regulator in HB-EGF/EGFR signaling–mediated KC migration and wound closure. This study presents basic information about the role played by nuclear IL-33 in human KC migration, which contributes to our understanding of skin wound healing.

METHODS AND MATERIALS

KC culture and treatment

This study was conducted according to the principles of the Declaration of Helsinki, and all procedures involving human subjects received previous approval from the Ethics Committee at Ehime

University School of Medicine (Ehime, Japan). Normal human skin biopsies were obtained from plastic surgeries. All participants provided written informed consent. The epidermis was separated from the dermis, and NHEKs were collected and cultured under serum-free conditions, MCDB medium, as previously described (Shirakata et al., 2004). The subconfluent cultures of NHEKs that had been passaged four times were treated with recombinant HB-EGF together with buffer or specific inhibitors, such as U0126 (10 μM, R&D Systems, Minneapolis, MN) and AG 1478 (3 μM), Bay 11-7082 (10 μM), and wortmannin (10 μM) (Calbiochem, Tokyo, Japan) for different times. In some experiments, cells were transfected with siRNAs or infected with an Ax.

siRNA or Ax

The stealth siRNA for human IL-33 (HSS132062) and its scrambled siRNA (number 12935112) were obtained from Thermo Fisher Scientific (Yokohama, Japan). ON-TARGETplus human NFKB1 (p65) siRNA (L-003520-00) and ON-TARGETplus nontargeting siRNA (D-0031810-01-20) were obtained from Thermo Fisher Scientific Dharmacon (Lafayette, CO). The cultures of NHEKs at about 60% confluence were transfected with siRNA using Lipofectamine RNAiMAX Transfection Reagent (Thermo Fisher Scientific), according to the manufacturer's instructions. The cells were allowed to stabilize for at least 48 hours before using them for further experiments.

Axs expressing the dominant-negative form of STAT3 (STAT3F-expressing Ax) were prepared and introduced into KCs at a multiplicity of infection = 10 as described previously (Dai et al., 2006; Yamasaki et al., 2003), and LacZ-expressing Ax was used as a control. The cells were allowed to stabilize for 24 hours before being used for further experiments.

RNA preparation and real-time RT-PCR

The probes specific for IL-33 (Hs04931857_m1), MMP1 (Hs00899658_m1), MMP3 (Hs00968305_m1), MMP9 (Hs00234579_m1), MMP10 (Hs00233987_m1), K1 (Hs00196158_m1), K10 (Hs00166289_m1), and human endogenous control (4310857) were obtained from Thermo Fisher Scientific. Total RNA was isolated and subjected to real-time RT-PCR, and gene expression was analyzed, as described previously (Dai et al., 2006).

Protein isolation and western blotting

Total cytoplasmic and nuclear cell extracts were collected at the indicated times after stimulation. The whole-cell extracts were collected using RIPA buffer (Wako, Tokyo, Japan). NE-PER Nuclear and Cytoplasmic Extraction Reagents (Thermo Fisher Scientific) were used to separate nuclear extracts from cytoplasmic extracts, according to the instructions. The proteins were separated by SDS-PAGE and transferred to polyvinylidene difluoride membranes. Analyses were performed using a Vistra ECF Kit (Amersham Biosciences, Arlington Heights, IL), and then membranes were scanned using a FluorImager (Molecular Dynamics, Sunnyvale, CA). In some graphs, the quantitative analysis of protein expression (band intensity) was performed using ImageJ software (National Institutes of Health, Bethesda, MD) from three independent experiments, and the graphs indicating the relative protein levels were shown together with the protein bands. The primary antibodies used for western blotting are listed in Table 1.

KCs expressing c-Myc−IL-33

Human *IL33* gene open reading frame cDNA clone expression plasmid, c-Myc tag (pc-Myc−IL-33) was obtained from Sino Biological (Beijing, China, catalog number HG10368-CM). The plasmid has been confirmed by full-length sequencing. Subconfluent KCs were transfected with pc-Myc−IL-33 (~0−2 mg/10^6 cells) using FuGENE 4k Transfection Reagent (Promega, Madison, WI), according to the manufacturer's instructions, as described in our previous report (Dai et al., 2022b). The cells were stabilized for 24 hours before being exposed to HB-EGF.

Coimmunoprecipitation assay

The protocol provided by the manufacturers was followed, with minor modifications. For immunoprecipitation of p-STAT3, IL-33, or Myc (Table 1), the nuclei pellets (obtained as described earlier) were lysed in a nondenaturing lysis buffer (20 mM Tris hydrogen chloride at pH 8.0, 137 mM sodium chloride, 1% Triton X-100, and 2 mM EDTA), and sepharose G beads were used. After immunoprecipitation, the samples were washed three times with RIPA buffer. After the final wash, the pellets were suspended in 2× SDS sample buffer, boiled for 3 minutes, and separated together with the input sample by SDS-PAGE. The immunoblotting of IL-33, p-STAT3, and Myc was performed.

Chromatin immunoprecipitation-qPCR assay

After stimulation with HB-EGF for 15 hours, NHEKs were treated with 1% formaldehyde for 10 minutes at room temperature. The cells were harvested and subjected to chromatin immunoprecipitation using SimpleChIP Enzymatic Chromatin IP Kit (Cell Signaling Technology, Danvers, MA) according to the instructions. After chromatin immunoprecipitation with anti−p-STAT3 or antihistone H3 (an assay control) (Table 1), the captured genomic fragments were recovered by phenol-chloroform extraction. To exclude the nonspecific binding of antibodies, chromatin complexes were also immunoprecipitated with an anti-IgG antibody as a negative control. Identification of the MMP9 promoter fragments was performed by qPCR using primers designed on the basis of the STAT3-binding sequence in the MMP9 promoter (Jia et al., 2017). FastStart Universal SYBR Green Master (Sigma-Aldrich, Tokyo, Japan) was used to quantitate PCR products.

Electrophoretic mobility shift assay

Nuclear extracts were isolated using NE-PER Nuclear and Cytoplasmic Extraction Reagents (Thermo Fisher Scientific). Electrophoretic mobility shift assay was performed using a LightShift Chemiluminescent EMSA Kit (Thermo Fisher Scientific) and oligonucleotide probe sets specific for NF-κB (Panomics, Redwood City, CA) according to the manufacturer's instructions, as described previously (Dai et al., 2010).

In vivo mice wound and wound skin sections

Female C57BL/6JJcl mice (CLEA Japan, Tokyo, Japan) aged ~8 weeks were used for the generation of in vivo skin wounds. Under sodium pentobarbital anesthesia, the hair was shaved, and full-thickness skin wounds were created on the back of mice using 6-mm skin biopsy punches. The skins of wound margins were harvested for paraffin or frozen sections 0, 1, 2, 3, and 4 days after wounding.

Immunohistochemistry

The mouse skin sections were deparaffinized, antigen unmasked (or not), incubated in 3% hydrogen peroxide to block endogenous peroxidase, and reacted with primary antibodies (Table 1) overnight at 4 °C, according to the instructions of the manufacturers. The slides were treated with secondary antibodies conjugated with horseradish peroxidase (Nichirei Biosciences, Tokyo, Japan). Images were

Table 1. List of Primary Antibodies Used in this Study

Name of Antibodies	Catalog Number	Providers	Usages (Dilution)
EGFR (A-10)	sc-373746	Santa Cruz Biotechnology (Dallas, TX)	Western blotting (1/1,000)
Phosphorylated EGFR (Tyr1068) D7A5 XP	3777	Cell Signaling Technology (Danvers, MA)	Western blotting (1/1,000) Immunohistochemistry (1/100)
Phosphorylated p44/42 MAPK (ERK1/2)	9101	Cell Signaling Technology (Danvers, MA)	Western blotting (1/1,000) Immunohistochemistry (1/100)
p44/42 MAPK (ERK1/2)	9102	Cell Signaling Technology (Danvers, MA)	Western blotting (1/1,000)
STAT3	9139	Cell Signaling Technology (Danvers, MA)	Western blotting (1/1,000)
Phosphorylated STAT3 (Tyr705)	9145	Cell Signaling Technology (Danvers, MA)	ChIP assay (1/400) Immunoprecipitation (1/400) Immunohistochemistry (1/100) Immunofluorescence (1/100)
IL-33	PM033	MBL (Tokyo, Japan))	Western blotting (1/1,000) Immunohistochemistry (1/1,000) Immunofluorescence (1/200)
IL-33	sc-130625	Santa Cruz Biotechnology (Dallas, TX)	Western blotting (1/500, for immunoprecipitation samples) Immunoprecipitation (1/100)
Phosphorylated Akt (Ser473)	9271	Cell Signaling Technology (Danvers, MA)	Western blotting (1/1,000)
Akt	9272	Cell Signaling Technology (Danvers, MA)	Western blotting (1/1,000)
Anti-MMP9 antibody (EP1254)	ab76003	Abcam (Tokyo, Japan)	Western blotting (1/1,000)
Cytokeratin 1 (E-12)	sc-376224	Santa Cruz Biotechnology (Dallas, TX)	Western blotting (1/500)
Cytokeratin 1–specific antibody.	16848-1-AP	ProteinTech (Tokyo, Japan))	Immunohistochemistry (1/200)
Keratin 10 Ab-2	MS-611-P1	Thermo Fisher Scientific (Yokohama, Japan)	Western blotting (1/500)
Cytokeratin 10–specific antibody.	18343-1-AP	ProteinTech (Tokyo, Japan))	Immunohistochemistry (1/1,000)
NF-kB p65 XP	8242	Cell Signaling Technology (Danvers, MA)	Western blotting (1/1,000)
Phosphorylated NF-κB p65 (Ser726) Antibody	3037	Cell Signaling Technology (Danvers, MA)	Western blotting (1/1,000)
Histone H3	2650	Cell Signaling Technology (Danvers, MA)	ChIP assay (1/400)
Lamin A	613501	BioLegend (San Diego, CA)	Western blotting (1/200)
β-Actin	ab6276	Abcam (Tokyo, Japan)	Western blotting (1/1,0000)
Anti-Myc Tag Antibody	05-419	Upstate (Tokyo, Japan)	Immunoprecipitation (1/100) Western blotting (1/1,000)

Abbreviations: Akt, protein kinase B; ChIP, chromatin immunoprecipitation; ERK, extracellular signal–regulated kinase; STAT, signal transducer and activator of transcription;

photographed using a BZ-X710 All-in-One fluorescence microscope (Keyence, Osaka, Japan). Control staining with IgG isotype yielded no positive signal.

Confocal immunofluorescence microscopy

KCs or frozen mouse skin sections were fixed with 4% paraformaldehyde, incubated overnight at 4 °C with antibodies raised against IL-33 or p-STAT3 (Table 1), and then treated with an Alexa Fluor 488–conjugated secondary antibody (Thermo Fisher Scientific) together with DAPI (Invitrogen, Carlsbad, CA), as described previously (Dai et al., 2011). The slides were washed with PBS and mounted using VECTASHIED (Vector Laboratories, Burlingame, CA). Images were acquired using a Zeiss LSM 510 confocal laser scanning microscope (Carl Zeiss, Jena, Germany). Control staining with IgG isotype controls or without primary antibodies yielded no positive signal.

Scratch wound healing assay

After NHEKs were grown to almost confluent, the cultures were scratched using sterile 6-mm or 8-mm scrapers, washed twice with PBS, and incubated in unsupplemented media containing HB-EGF with or without inhibitors. Cell cultures were recorded after scratching, and the percentage of unrecovered wound area at the indicated time (compared with that at the 0 hours uncovered wound area, 100%) was calculated by ImageJ software (National Institutes of Health). Similar results were obtained from three individual experiments. In some experiments, the cells were infected with Ax or transfected with siRNA before being subjected to scratching. In some experiments, the cultures were treated with HB-EGF or IL-33 (100 ng/ml, R&D Systems) with or without recombinant human ST2/IL-33R Fc chimera protein (300 ng/ml, R&D Systems) or batimastat (10 μM, Calbiochem).

Boyden chamber migration assay

KC migration was assayed quantitatively using a 48-well Boyden chamber (Neuro Probe, Tokyo, Japan), as described in our previous report (Tokumaru et al., 2005). To investigate the involvement of nuclear IL-33 or STAT3 activation in HB-EGF–induced KC migration, siRNA-transfected cells or Ax-infected cells were collected and added into the upper wells of the chamber, whereas HB-EGF together with or without specific inhibitors were added into the bottom wells of the chamber.

ELISA

After scratching or without scratching, the culture supernatants were respectively collected and stored at −20 °C before use. Supernatant IL-33 levels were quantified using a commercially available IL-33 ELISA kit (R&D Systems), according to the manufacturer's instructions.

Nano-Glo luciferase assay

We obtained the pNL3.2.NF-κB-RE[NlucP/NF-κB-RE/Hygro] vector from Promega, which contained five copies of an NF-κB response element (i.e., NF-κB-RE) that drives transcription of a destabilized form of NanoLuc luciferase. After transfection with siRNA for 24 hours, KCs at ∼75% confluency were transfected with pNL3.2.NF-κB-RE vector using FuGENE HD transfection reagent (Promega), according to the manufacturer's instructions. The cells were stabilized for a 24-hours recovery time for lipid-mediated transfections before being exposed to HB-EGF. The NF-κB−responsive luciferase activity was analyzed using the Nano-Glo Luciferase Assay System (Promega), according to the manufacturer's instructions. The relative fold induction of luciferase activity was calculated and determined as described previously (Dai et al., 2021).

Statistical analysis

At least three independent experiments were performed, all of which yielded similar results for each test, with the representative one presented. To present each quantitative data point clearly, we prepared the dot plots using GraphPad Prism 9.5.0 (GraphPad Software, San Diego, CA). Each data shown in the figure represent the results of a single experiment (except the quantitative data of protein expression), with 3−6 samples per test point, and the dots in the graph indicate the values of these ∼3−6 samples for each test point. The uncovered wound area was calculated by ImageJ 1.53t (National Institutes of Health) and compared with that just after scratching (0 hours), with the 0-hour uncovered wound area being 100%. The protein bands were quantified by ImageJ 1.53t to correct protein loading discrepancies, the protein levels of the treated group were obtained relative to the control group, and the data from three individual experiments are shown in the dot plot to indicate the relative protein levels. The quantitative data are expressed as mean ± SD ($n \geq 3$). Comparisons were analyzed with repeated-measures ANOVA (one-way ANOVA with Dunnett test or two-way ANOVA followed by Bonferroni corrections) or using a paired Student *t*-test, and type I error was adjusted for multiple testing. Analysis was done with IBM Statistical Package for the Social Sciences Statistics 25 (IBM, New York City, NY). The level of statistical significance was set to $P < 0.05$, $P < 0.01$, and $P < 0.001$.

Data availability statement

No large datasets were generated or analyzed during this study. Minimal datasets necessary to interpret or replicate data in this paper are available upon request to the corresponding author.

ORCIDs

Xiuju Dai: http://orcid.org/0000-0002-1487-7466
Ken Shiraishi: http://orcid.org/0000-0002-1153-7749
Jun Muto: http://orcid.org/0000-0001-9565-9796
Hideki Mori: http://orcid.org/0000-0002-7323-6466
Masamoto Murakami: http://orcid.org/0000-0003-3923-5096
Koji Sayama: http://orcid.org/0000-0001-9915-8964

CONFLICT OF INTEREST

The authors state no conflict of interest.

ACKNOWLEDGMENTS

This work was supported by a general research grant from Pfizer (Pfizer #67455113). We thank Teruko Tsuda and Eriko Tan for their technical assistance.

AUTHOR CONTRIBUTIONS

Conceptualization: XD, KS, JM, HM, MM, KS; Data Curation: XD, KS; Formal Analysis: XD, KS; Funding Acquisition: XD; Investigation: XD; Methodology: XD, KS, JM, HM, MM, KS; Project Administration: XD, KS; Resources: XD; Visualization: XD; Writing − Original Draft Preparation: XD; Writing − Review and Editing: XD, KS, JM, HM, MM, KS

REFERENCES

Ali S, Mohs A, Thomas M, Klare J, Ross R, Schmitz ML, et al. The dual function cytokine IL-33 interacts with the transcription factor NF-κB to dampen NF-κB-stimulated gene transcription. J Immunol 2011;187:1609−16.

Baekkevold ES, Roussigné M, Yamanaka T, Johansen FE, Jahnsen FL, Amalric F, et al. Molecular characterization of NF-HEV, a nuclear factor preferentially expressed in human high endothelial venules. Am J Pathol 2003;163:69−79.

Balato A, Raimondo A, Balato N, Ayala F, Lembo S. Interleukin-33: increasing role in dermatological conditions. Arch Dermatol Res 2016;308:287−96.

Block ER, Tolino MA, Klarlund JK. Extracellular ATP stimulates epithelial cell motility through Pyk2-mediated activation of the EGF receptor. Cell Signal 2011;23:2051−5.

Boucher I, Kehasse A, Marcincin M, Rich C, Rahimi N, Trinkaus-Randall V. Distinct activation of epidermal growth factor receptor by UTP contributes to epithelial cell wound repair. Am J Pathol 2011;178:1092−105.

Carriere V, Roussel L, Ortega N, Lacorre DA, Americh L, Aguilar L, et al. IL-33, the IL-1-like cytokine ligand for ST2 receptor, is a chromatin-associated nuclear factor in vivo. Proc Natl Acad Sci USA 2007;104:282−7.

Cheng CY, Kuo CT, Lin CC, Hsieh HL, Yang CM. IL-1beta induces expression of matrix metalloproteinase-9 and cell migration via a c-Src-dependent, growth factor receptor transactivation in A549 cells. Br J Pharmacol 2010;160:1595−610.

Dai X, Murakami M, Shiraishi K, Muto J, Tohyama M, Mori H, et al. EGFR ligands synergistically increase IL-17A-induced expression of psoriasis signature genes in human keratinocytes via IκBζ and Bcl3. Eur J Immunol 2022a;52:994−1005.

Dai X, Muto J, Shiraishi K, Utsunomiya R, Mori H, Murakami M, et al. TSLP impairs epidermal barrier integrity by stimulating the formation of nuclear IL-33/phosphorylated STAT3 complex in human keratinocytes. J Invest Dermatol 2022b;142:2100−8.e5.

Dai X, Sayama K, Tohyama M, Shirakata Y, Hanakawa Y, Tokumaru S, et al. PPARγ mediates innate immunity by regulating the 1α,25-dihydroxyvitamin D3 induced hBD-3 and cathelicidin in human keratinocytes. J Dermatol Sci 2010;60:179−86.

Dai X, Sayama K, Tohyama M, Shirakata Y, Hanakawa Y, Tokumaru S, et al. Mite allergen is a danger signal for the skin via activation of inflammasome in keratinocytes. J Allergy Clin Immunol 2011;127:806−14. e1-4.

Dai X, Sayama K, Yamasaki K, Tohyama M, Shirakata Y, Hanakawa Y, et al. SOCS1-negative feedback of STAT1 activation is a key pathway in the dsRNA-induced innate immune response of human keratinocytes. J Invest Dermatol 2006;126:1574−81.

Dai X, Shiraishi K, Muto J, Utsunomiya R, Mori H, Murakami M, et al. Nuclear IL-33 plays an important role in IL-31−mediated downregulation of FLG, keratin 1, and keratin 10 by regulating signal transducer and activator of transcription 3 activation in human keratinocytes. J Invest Dermatol 2022c;142:136−44.e3.

Dai X, Tohyama M, Murakami M, Shiraishi K, Liu S, Mori H, et al. House dust mite allergens induce interleukin 33 (IL-33) synthesis and release from keratinocytes via ATP-mediated extracellular signaling. Biochim Biophys Acta Mol Basis Dis 2020;1866:165719.

Dai X, Utsunomiya R, Shiraishi K, Mori H, Muto J, Murakami M, et al. Nuclear IL-33 plays an important role in the suppression of FLG, LOR, keratin 1, and keratin 10 by IL-4 and IL-13 in human keratinocytes. J Invest Dermatol 2021;141:2646−55.e6.

Dickel H, Gambichler T, Kamphowe J, Altmeyer P, Skrygan M. Standardized tape stripping prior to patch testing induces upregulation of Hsp90, Hsp70,

IL-33, TNF-α and IL-8/CXCL8 mRNA: new insights into the involvement of 'alarmins'. Contact Dermatitis 2010;63:215–22.

Fukushi S, Yamasaki K, Aiba S. Nuclear localization of activated STAT6 and STAT3 in epidermis of prurigo nodularis. Br J Dermatol 2011;165:990–6.

Gallucci RM, Sloan DK, Heck JM, Murray AR, O'Dell SJ. Interleukin 6 indirectly induces keratinocyte migration. J Invest Dermatol 2004;122:764–72.

Gordon GM, Ledee DR, Feuer WJ, Fini ME. Cytokines and signaling pathways regulating matrix metalloproteinase-9 (MMP-9) expression in corneal epithelial cells. J Cell Physiol 2009;221:402–11.

Heilborn JD, Nilsson MF, Kratz G, Weber G, Sørensen O, Borregaard N, et al. The cathelicidin anti-microbial peptide LL-37 is involved in re-epithelialization of human skin wounds and is lacking in chronic ulcer epithelium. J Invest Dermatol 2003;120:379–89.

Imai Y. Interleukin-33 in atopic dermatitis. J Dermatol Sci 2019;96:2–7.

Jia ZH, Jia Y, Guo FJ, Chen J, Zhang XW, Cui MH. Phosphorylation of STAT3 at Tyr705 regulates MMP-9 production in epithelial ovarian cancer. PLoS One 2017;12:e0183622.

Jiang L, Shao Y, Tian Y, Ouyang C, Wang X. Nuclear alarmin cytokines in inflammation. J Immunol Res 2020;2020:7206451.

Jin M, Komine M, Tsuda H, Oshio T, Ohtsuki M. dsRNA induces IL-33 promoter activity through TLR3-EGFR-IRF3 pathway in normal human epidermal keratinocytes. J Dermatol Sci 2019;96:178–80.

Jost M, Kari C, Rodeck U. The EGF receptor - an essential regulator of multiple epidermal functions. Eur J Dermatol 2000;10:505–10.

Kajanne R, Miettinen P, Mehlem A, Leivonen SK, Birrer M, Foschi M, et al. EGF-R regulates MMP function in fibroblasts through MAPK and AP-1 pathways. J Cell Physiol 2007;212:489–97.

Kochupurakkal BS, Harari D, Di-Segni A, Maik-Rachline G, Lyass L, Gur G, et al. Epigen, the last ligand of ErbB receptors, reveals intricate relationships between affinity and mitogenicity. J Biol Chem 2005;280:8503–12.

Kyriakides TR, Wulsin D, Skokos EA, Fleckman P, Pirrone A, Shipley JM, et al. Mice that lack matrix metalloproteinase-9 display delayed wound healing associated with delayed reepithelization and disordered collagen fibrillogenesis. Matrix Biol 2009;28:65–73.

Legrand C, Gilles C, Zahm JM, Polette M, Buisson AC, Kaplan H, et al. Airway epithelial cell migration dynamics. MMP-9 role in cell-extracellular matrix remodeling. J Cell Biol 1999;146:517–29.

Marikovsky M, Breuing K, Liu PY, Eriksson E, Higashiyama S, Farber P, et al. Appearance of heparin-binding EGF-like growth factor in wound fluid as a response to injury. Proc Natl Acad Sci USA 1993;90:3889–93.

Martins VL, Caley M, O'Toole EA. Matrix metalloproteinases and epidermal wound repair. Cell Tissue Res 2013;351:255–68.

Mathay C, Giltaire S, Minner F, Bera E, Hérin M, Poumay Y. Heparin-binding EGF-like growth factor is induced by disruption of lipid rafts and oxidative stress in keratinocytes and participates in the epidermal response to cutaneous wounds. J Invest Dermatol 2008;128:717–27.

Mathay C, Pierre M, Pittelkow MR, Depiereux E, Nikkels AF, Colige A, et al. Transcriptional profiling after lipid raft disruption in keratinocytes identifies critical mediators of atopic dermatitis pathways. J Invest Dermatol 2011;131:46–58.

McCawley LJ, O'Brien P, Hudson LG. Epidermal growth factor (EGF)- and scatter factor/hepatocyte growth factor (SF/HGF)- mediated keratinocyte migration is coincident with induction of matrix metalloproteinase (MMP)-9. J Cell Physiol 1998;176:255–65.

Meephansan J, Komine M, Tsuda H, Karakawa M, Tominaga S, Ohtsuki M. Expression of IL-33 in the epidermis: the mechanism of induction by IL-17. J Dermatol Sci 2013;71:107–14.

Meephansan J, Tsuda H, Komine M, Tominaga S, Ohtsuki M. Regulation of IL-33 expression by IFN-γ and tumor necrosis factor-α in normal human epidermal keratinocytes. J Invest Dermatol 2012;132:2593–600.

Moussion C, Ortega N, Girard JP. The IL-1-like cytokine IL-33 is constitutively expressed in the nucleus of endothelial cells and epithelial cells in vivo: a novel 'alarmin'? PLoS One 2008;3:e3331.

Na J, Lee K, Na W, Shin JY, Lee MJ, Yune TY, et al. Histone H3K27 demethylase JMJD3 in cooperation with NF-κB regulates keratinocyte wound healing. J Invest Dermatol 2016;136:847–58.

Nabe T. Interleukin (IL)-33: new therapeutic target for atopic diseases. J Pharmacol Sci 2014;126:85–91.

Niyonsaba F, Ushio H, Nakano N, Ng W, Sayama K, Hashimoto K, et al. Antimicrobial peptides human beta-defensins stimulate epidermal keratinocyte migration, proliferation and production of proinflammatory cytokines and chemokines. J Invest Dermatol 2007;127:594–604.

Nomura K, Kojima T, Fuchimoto J, Obata K, Keira T, Himi T, et al. Regulation of interleukin-33 and thymic stromal lymphopoietin in human nasal fibroblasts by proinflammatory cytokines. Laryngoscope 2012;122:1185–92.

Oshio T, Komine M, Tsuda H, Tominaga SI, Saito H, Nakae S, et al. Nuclear expression of IL-33 in epidermal keratinocytes promotes wound healing in mice. J Dermatol Sci 2017;85:106–14.

Pastore S, Mascia F, Mariani V, Girolomoni G. The epidermal growth factor receptor system in skin repair and inflammation. J Invest Dermatol 2008;128:1365–74.

Pietka W, Khnykin D, Bertelsen V, Lossius AH, Stav-Noraas TE, Hol Fosse J, et al. Hypo-osmotic stress drives IL-33 production in human keratinocytes-an epidermal homeostatic response. J Invest Dermatol 2019;139:81–90.

Poumay Y, de Rouvroit CL. HB-EGF, the growth factor that accelerates keratinocyte migration, but slows proliferation. J Invest Dermatol 2012;132:2129–30.

Roepstorff K, Grandal MV, Henriksen L, Knudsen SL, Lerdrup M, Grøvdal L, et al. Differential effects of EGFR ligands on endocytic sorting of the receptor. Traffic 2009;10:1115–27.

Rousselle P, Montmasson M, Garnier C. Extracellular matrix contribution to skin wound re-epithelialization. Matrix Biol 2019;75–76:12–26.

Sano S, Itami S, Takeda K, Tarutani M, Yamaguchi Y, Miura H, et al. Keratinocyte-specific ablation of Stat3 exhibits impaired skin remodeling, but does not affect skin morphogenesis. EMBO J 1999;18:4657–68.

Savinko T, Matikainen S, Saarialho-Kere U, Lehto M, Wang G, Lehtimäki S, et al. IL-33 and ST2 in atopic dermatitis: expression profiles and modulation by triggering factors. J Invest Dermatol 2012;132:1392–400.

Sharma S, Kulk N, Nold MF, Gräf R, Kim SH, Reinhardt D, et al. The IL-1 family member 7b translocates to the nucleus and down-regulates proinflammatory cytokines. J Immunol 2008;180:5477–82.

Shirakata Y, Kimura R, Nanba D, Iwamoto R, Tokumaru S, Morimoto C, et al. Heparin-binding EGF-like growth factor accelerates keratinocyte migration and skin wound healing. J Cell Sci 2005;118:2363–70.

Shirakata Y, Komurasaki T, Toyoda H, Hanakawa Y, Yamasaki K, Tokumaru S, et al. Epiregulin, a novel member of the epidermal growth factor family, is an autocrine growth factor in normal human keratinocytes. J Biol Chem 2000;275:5748–53.

Shirakata Y, Tokumaru S, Sayama K, Hashimoto K. Auto- and cross-induction by betacellulin in epidermal keratinocytes. J Dermatol Sci 2010;58:162–4.

Shirakata Y, Ueno H, Hanakawa Y, Kameda K, Yamasaki K, Tokumaru S, et al. TGF-beta is not involved in early phase growth inhibition of keratinocytes by 1alpha,25(OH)2vitamin D3. J Dermatol Sci 2004;36:41–50.

Song Y, Qian L, Song S, Chen L, Zhang Y, Yuan G, et al. Fra-1 and Stat3 synergistically regulate activation of human MMP-9 gene. Mol Immunol 2008;45:137–43.

Stoll S, Garner W, Elder J. Heparin-binding ligands mediate autocrine epidermal growth factor receptor activation in skin organ culture. J Clin Invest 1997;100:1271–81.

Stoll SW, Johnson JL, Bhasin A, Johnston A, Gudjonsson JE, Rittié L, et al. Metalloproteinase-mediated, context-dependent function of amphiregulin and HB-EGF in human keratinocytes and skin. J Invest Dermatol 2010;130:295–304.

Stoll SW, Rittié L, Johnson JL, Elder JT. Heparin-binding EGF-like growth factor promotes epithelial-mesenchymal transition in human keratinocytes. J Invest Dermatol 2012;132:2148–57.

Stoscheck CM, Nanney LB, King LE Jr. Quantitative determination of EGF-R during epidermal wound healing. J Invest Dermatol 1992;99:645–9.

Sundnes O, Pietka W, Loos T, Sponheim J, Rankin AL, Pflanz S, et al. Epidermal expression and regulation of interleukin-33 during homeostasis and inflammation: strong species differences. J Invest Dermatol 2015;135:1771–80.

Tokumaru S, Higashiyama S, Endo T, Nakagawa T, Miyagawa JI, Yamamori K, et al. Ectodomain shedding of epidermal growth factor receptor ligands is required for keratinocyte migration in cutaneous wound healing. J Cell Biol 2000;151:209–20.

Tokumaru S, Sayama K, Shirakata Y, Komatsuzawa H, Ouhara K, Hanakawa Y, et al. Induction of keratinocyte migration via transactivation of the epidermal growth factor receptor by the antimicrobial peptide LL-37. J Immunol 2005;175:4662–8.

Uchiyama A, Nayak S, Graf R, Cross M, Hasneen K, Gutkind JS, et al. SOX2 epidermal overexpression promotes cutaneous wound healing via activation of EGFR/MEK/ERK signaling mediated by EGFR ligands. J Invest Dermatol 2019;139:1809–20.e8.

Vageli DP, Exarchou A, Zafiriou E, Doukas PG, Doukas S, Roussaki-Schulze A. Effect of TNF-α inhibitors on transcriptional levels of pro-inflammatory interleukin-33 and Toll-like receptors-2 and -9 in psoriatic plaques. Exp Ther Med 2015;10:1573–7.

Wang Z. Transactivation of epidermal growth factor receptor by G protein-coupled receptors: recent progress, challenges and future research. Int J Mol Sci 2016;17:95.

Wilson KC, Center DM, Cruikshank WW. The effect of interleukin-16 and its precursor on T lymphocyte activation and growth. Growth Factors 2004;22:97–104.

Wulff BC, Pappa NK, Wilgus TA. Interleukin-33 encourages scar formation in murine fetal skin wounds. Wound Repair and Regen 2019;27:19–28.

Xiang Y, Li JP, Guo W, Wang DQ, Yao A, Zhang HM, et al. Novel interactions between ERα-36 and STAT3 mediate breast cancer cell migration. Cell Commun Signal 2019;17:93.

Yamasaki K, Hanakawa Y, Tokumaru S, Shirakata Y, Sayama K, Hanada T, et al. Suppressor of cytokine signaling 1/JAB and suppressor of cytokine signaling 3/cytokine-inducible SH2 containing protein 3 negatively regulate the signal transducers and activators of transcription signaling pathway in normal human epidermal keratinocytes. J Invest Dermatol 2003;120:571–80.

Yin J, Xu K, Zhang J, Kumar A, Yu FS. Wound-induced ATP release and EGF receptor activation in epithelial cells. J Cell Sci 2007;120:815–25.

Yu XX, Hu Z, Shen X, Dong LY, Zhou WZ, Hu WH. IL-33 promotes gastric cancer cell invasion and migration via ST2-ERK1/2 pathway. Dig Dis Sci 2015;60:1265–72.

This work is licensed under a Creative Commons Attribution-NonCommercial-NoDerivatives 4.0 International License. To view a copy of this license, visit http://creativecommons.org/licenses/by-nc-nd/4.0/